Department of Electrical Engineering and Computer Science

TEMPUS PROJECT JEP 7403-94

Wideband Analysis of the Propagation Channel in Mobile Broadband System

Krzysztof Jacek Kurek

Final report

Supervisor: Prof. Luis Correia

July 1997
Lisbon, Portugal

Acknowledgments

I wish to thank Professor Luis Correia for his help, advice and supervision of my work

Abstract

This report presents an analysis of the wideband propagation channel in Mobile Broadband System, for a typical scenario of this system: an urban street with buildings on both sides. The analysis is based on simulations, by using a ray-tracing tool previously developed. The signal propagation within the street is modeled by Geometrical Optics, accounting for reflections up to the third order. The mean delay and delay spread along the street are used to characterize the propagation channel. It is observed that these parameters are a function of street's width, walls' roughness, receiver's bandwidth, and type of antennas, among other parameters. An analytical approximation for these dependencies is presented.

Keywords

Mobile Broadband System, multipath propagation channel, power delay profile, delay spread

Table of contents

Acknowledgments ..... **i**

Abstract ..... **ii**

Keywords ..... **ii**

Table of contents ..... **iii**

List of Figures ..... **iv**

List of Tables ..... **vi**

List of symbols ..... **vii**

List of Acronyms ..... **ix**

1. Introduction **1**

2. Theoretical aspects of signal propagation in mobile systems **3**

2.1 Mobile multipath propagation channel 3

2.1.1 Channel description *3*

2.1.2 Time dispersion *7*

2.1.3 Time variation of the channel *11*

2.2 Modeling of the multipath propagation channel 12

2.3 Propagation channel at the 60 GHz band 16

2.3.1 Signal attenuation *16*

2.3.2 Model for the signal propagation *18*

3. Analysis of results from simulations **22**

3.1 Simulation scenario 22

3.2 Dependence on system bandwidth 26

3.3 Dependence on walls materials 30

3.4 Dependence on the roughness of reflecting surfaces 31

3.5 Dependence on the width of the street 34

3.6 Dependence on the length of the street 36

3.7 Dependence on base and mobile stations position 38

3.8 Dependence on base and mobile stations antennas' heights 43

3.9 Dependence on antennas types 46

3.10 Dependence on traffic in the street 48

4. Conclusions **50**

Annex A. Radiation patterns of antennas used in simulations **52**

References **53**

List of Figures

Figure 2.1 Multipath propagation environment 3
Figure 2.2 Ilustration of Doppler effect 4
Figure 2.3 The time varing discrete-time impulse response of the multipath channel 7
Figure 2.4 Power delay profile 8
Figure 2.5 Flat fading characteristics in time and frequency domains 10
Figure 2.6 Frequency selective fading characteristics in time and frequency domains 10
Figure 2.7 Probability density function of the Rayleigh distribution 13
Figure 2.8 Probability density function of the Rician distribution 15
Figure 2.9 Taped-delay line - model of the channel impulse response 15
Figure 2.10 Oxygen absorption and rain attenuation 17
Figure 3.1 Simulation scenario 22
Figure 3.2 Discrete delay profile of the standard street. 24
Figure 3.3 Continuous power delay profile for the standard street and its exponential approxymation 24
Figure 3.4 Ilustration of path length difference between LOS and wall reflected rays for a small and a large distance between the BS and the MS 25
Figure 3.5 Discrete power delay profile for different system bandwidths 27
Figure 3.6 Power delay profiles for different system bandwidths 28
Figure 3.7 Delay parameters as a function of system bandwidth 28
Figure 3.8 Approximation of delay parameters by hiperbolic tangents function of system bandwidth 29
Figure 3.9 Power delay profiles for different walls materials 30
Figure 3.10 Power delay profiles for different roughness of reflecting surfaces 31
Figure 3.11 Delay parameters for different roughness of reflecting surfaces 32
Figure 3.12 Approximation of delay parameters by exponential function of reflecting surfaces roughness 33
Figure 3.13 Power delay profiles for different streets widths 34
Figure 3.14 Delay parameters for different streets widths 35
Figure 3.15 Approximation of delay parameters by power function of the streets width 36
Figure 3.16 Power delay profiles for different streets lengths 36
Figure 3.17 Delay parameters for different streets lengths 37
Figure 3.18 Approximation of delay parameters by power function of the streets length 38
Figure 3.19 Power delay profiles for different BS positions 39
Figure 3.20 Delay parameters for different BS positions 40
Figure 3.21 Approximation of delay parameters by linear function of the BS position 41

Figure 3.22 Power delay profiles for different MS positions 41
Figure 3.23 Delay parameters for different MS positions 42
Figure 3.24 Power delay profiles for different BS antenna heights 43
Figure 3.25 Delay parameters for different BS antenna heights 44
Figure 3.26 Approximation of delay parameters by linear function of the BS antenna height 44
Figure 3.27 Power delay profiles for different MS antenna heights 45
Figure 3.28 Approximation of delay parameters by linear function of the MS antenna height 46
Figure 3.29 Power delay profiles for different types of BS and MS antennas 48
Figure 3.30 Power delay profiles for traffic in the street.....49
Figure A.1 Radiation patern of the MBS antenna used in simulations 52
Figure A.2 Radiation pattern of the directive antenna used in simulations.....52

List of Tables

Table 3.1 Delay parameters for the standard street 26
Table 3.2 Delay parameters for different system bandwidths 28
Table 3.3 Delay parameters for different walls materials 30
Table 3.4 Delay parameters for different roughness of reflecting surfaces.....32
Table 3.5 Delay parameters for different streets widths.....35
Table 3.6 Delay parameters for different streets lengths.....37
Table 3.7 Delay parameters for different BS positions 40
Table 3.8 Delay parameters for different MS positions 42
Table 3.9 Delay parameters for different BS antenna heights.....44
Table 3.10 Delay parameters for different MS antenna heights.....46
Table 3.11 Delay parameters for different types of BS and MS antennas 48
Table 3.12 Delay parameters for traffic in the street.....49
Table 4.1Considered scenario parameters and their influence on delay parameters.....50

List of symbols

B_c - *coherence bandwidth*

B_x - *system bandwidth*

$E_r(\theta_i)$ - *value of the receiver antenna pattern for the direction of i-th incoming component*

f_c - *carrier frequency*

f_D -*Doppler shift*

f_m - *maximum Doppler shift*

G_r - *receiver antenna gain*

G_t - *transmitter antenna gain*

$h(t,\tau)$ - *impulse response of time variant multipath propagation channel*

$h_b(t,\tau)$ - *equivalent lowpass impulse response of time variant multipath propagation channel*

N - *number of multipath components*

$P(t,\tau)$ - *power delay profile*

P_r - *received power*

P_t - *transmitted power*

$\tan\delta$ - *loss tangent*

T_c - *coherence time*

T_x - *symbol duration*

Z - *free space characteristic impedance*

α_i - *amplitude of i-th component*

Φ_i - *phase shift of i-th component*

$\varepsilon_r = \varepsilon_r' - j\varepsilon_r' \cdot \tan\delta$ -*complex relative dielectric constant*

ε_r' - *relative dielectric constant*

Γ - *Fresnel reflection coefficient*

γ - *parameter associated to the Rayleygh criterion of roughness*

γ_o - *attenuation coefficient for oxygen absorption*

γ_r - *rain attenuation coefficient*

λ - *wavelength*

σ_h - *surface's height standard deviation*

σ_τ - *delay spread*

θ - *incidence angle*

$\bar{\tau}$ -*mean excess delay*

τ_i - *delay of i-th component*

$\Delta\tau$ - *time resolution of the system*

v - *mobile velocity*

List of Acronyms

MBS - Mobile Broadband System

BER - Bit Error Rate

BS - Base Station

MS - Mobile Station

LOS - Line of Sight

GMSK - Gaussian Minimum Shift Key modulation

PDF - Probability Density Function

CDF - Cumulative Distribution Function

WSSUS - Wide-Sense Stationary Uncorrelated Scattering Channel

QWSSUS - Quasi-Wide-Sense Stationary Uncorrelated Scattering Channel

1. Introduction

Mobile communications systems give ability to communicate to users being in motion. Users can use them in different places and be independent of public fixed systems. The cellular concept, by using the same frequencies in spatially separated cells, allows to increase systems capacity. There are many new communication services being available for fixed and mobile users [1]:

1. digital data transmission
2. videotelephony
3. multimedia
4. moving pictures with high quality
5. teleworking, etc.

There is a trend in telecommunications to integrate in the future all these services in one system. In Europe, for mobile users, the Mobile Broadband System, MBS, will be such a system, giving its users access to all broadband services available in the future [2]. System performances, techniques and technology required for this system was the subject of the RACE II R2067 - MBS project [3]. It will be a cellular system with small cells, able to transmit with a data rate up to 155 Mb/s and working at the 60 GHz band. This band is chosen because:

1. There is an oxygen absorption peak in it, which it unusable for fixed communications systems, but appropriate for MBS, where the cells size is small. Additionally, the high attenuation of signals for large distances is a natural barrier to cochannel and adjacent channel interferences.
2. The relative bandwidth, necessary to the signal transmissions with such a high bit rate, is small.
3. The technological progress in microelectronics will allow to produce devices working in this band at a reasonable cost.

In mobile system design the propagation channel is a very important issue. This channel is quite different from the propagation in the free space and its parameters can vary in a large range in a short time. The signal arrives at the receiver as a large number of waves from different directions (multipath propagation), which can cause time dispersion and signal level variations. The received signal strength can vary more than 30 dB for small changes of the mobile position (less than 10 wavelength) [4]. For digital transmissions it can cause a

large increase of the bit error rate, BER, to a value of 10^{-2}, which is 10^6 times worse than in typical wire transmissions [4]. Additionally in mobile systems, the properties of the channel change in time due to the receiver or surrounding objects motion, which can cause signal distortion. Multipath propagation and receiver's motion impose fundamental limitations to the mobile system performance: the former leads to maximum and the latter minimum values of the signal bandwidth. In order to a mobile system to work properly in such disadvantageous conditions, the knowledge of these channel properties is necessary during the system design.

In this work it is presented a simple analysis of the mobile propagation channel in 60 GHz band, using a simple deterministic model. For these frequencies, wavelength is much smaller than the surrounding objects dimension, so the geometrical optics approach can be used for the signal propagation modeling. Simulations have shown which of system (types and height of the BS and MS antennas) and surrounding scenario (width, length of the street, buildings materials) parameters have the most influence on the properties of the propagation channel. In the second chapter it is presented the theoretical aspects of the signal propagation in mobile multipath channels and a short description of the method for the channel modeling. The last section of this chapter presents the geometrical optics description of the signal propagation at the 60 GHz band, which is used in simulations. Chapter 3 describes the simulation program and simulation assumptions, and presents the results from the simulation for different scenarios. The final chapter contains the conclusions.

2. Theoretical aspects of signal propagation in mobile systems

2.1 Mobile multipath propagation channel

2.1.1 Channel description

In mobile communications systems the signal transmitted by a base station, BS, arrives at the receiver as a large number of waves from different directions. This effect is called multipath propagation an it is caused by [5]:

1. Reflection from surrounding objects
2. Diffraction on sharp edges of objects
3. Scattering on rough surfaces

Due to the different delay, amplitude and phase of each multipath component, the received signal is different from the transmitted one, Fig.2.1, and can change with the position of the receiver or surrounding objects.

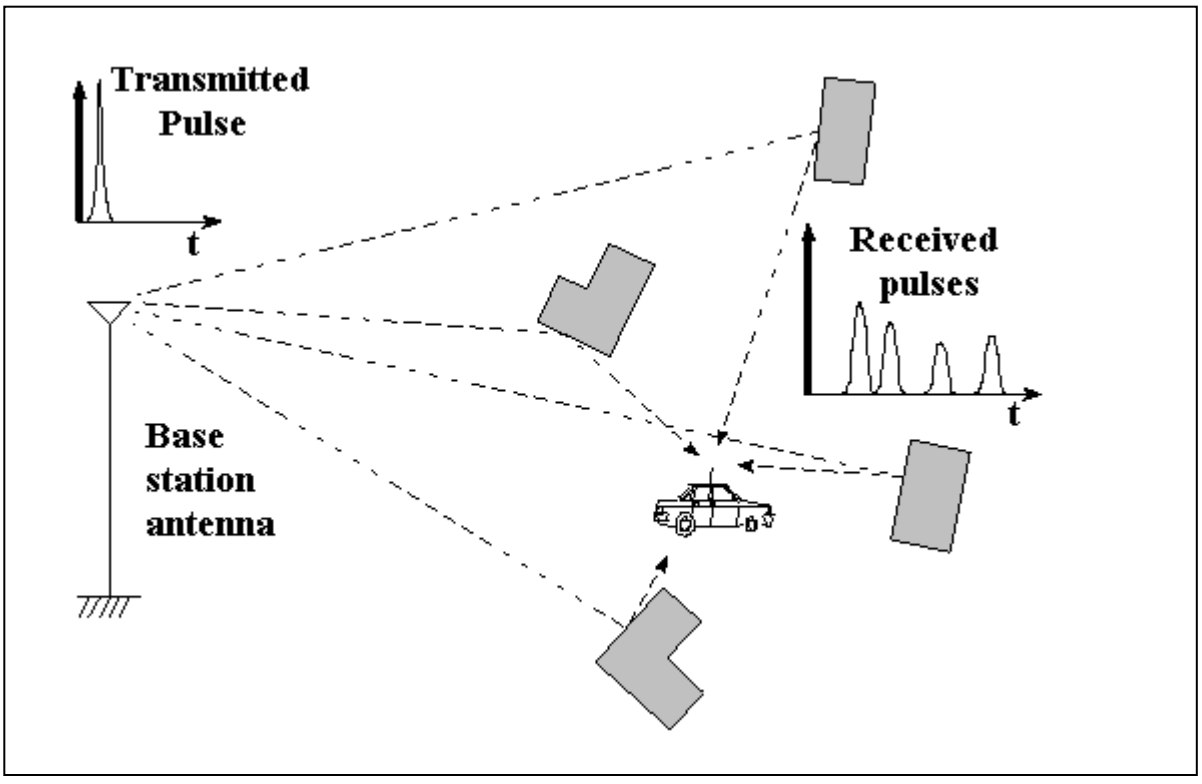

Figure 2.1 Multipath propagation environment (extracted from [6])

The multipath propagation channel can create the following effects in the received signal:

1. Rapid changes of the signal strength over a small distance or time. Variations of the signal amplitude occur because each multipath component has different phase, depending on the path length, so these components can be summed at receiver in a constructive or destructive way. It causes changes of the signal level larger than 20-30 dB when the receiver changes its position about one wavelength distance [7]. This effect is dominant for narrowband signals, in which case, from the receiver point of view, all signals components arrive at the same time (delay of multipath components can be neglected). For wideband signals, variations of the received signal power are smaller. The locations of the points where the signal fades depend on surrounding scenario objects and on the signal frequency. When the receiver is in a fade point, the communication between it and the BS may be impossible. To prevent losing the communication a fading margin in the transmitted power and diversity techniques are used[4]
2. Time dispersion of the received signal, due to the different delay of each multipath component, causing the received signal duration to be larger than the transmitted one. It can cause errors in wideband transmissions, when the time of the signal symbols repetition is smaller than the delays of the multipath components. In this case the MS receives at the same time one symbol and delayed echoes of previous one, intersymbol interference occurs and it is necessary to use an equalizer to receive a free error signal.

Figure 2.2 Ilustration of Doppler effect (extracted from [5])

Additionally in mobile systems the receiver position is not fixed. The relative motion between the base station and the receiver causes Doppler frequency shift, which is

proportional to the receiver velocity and to an angle between the direction of movement and the direction of an incoming wave, Fig.2.2.

The frequency shift is given by:

$$f_D = \frac{v}{\lambda}\cos\theta \tag{2.1}$$

where:

f_D - Doppler shift

v - mobile velocity

λ - wavelength

θ - angle as in Fig.2.2

The motion of the receiver through the multipath environment causes two effects [8]:

1. Frequency dispersion of the received signal. Each multipath component coming from various directions has different frequency shift, which causes a frequency stretching of the signal, specially visible for narrowband signals. That is to say, a harmonic signal is transmitted, but the received signal contains components in the band $[f_o - f_m, f_m + f_m]$, where f_o is transmitted frequency and f_m maximum Doppler shift. This frequency range is called Doppler spread B_D
2. Time variation of the channel properties. Due to the motion of the receiver through the multipath environment, the channel changes when the signal propagates. The channel seen by the leading edge of the symbol is not the same as the one seen by the trailing edge, and distortion of the signal can occur if this difference is large. For signals with short duration (wide band) these changes are not significant, but for signals with large duration the channel cannot be treated as constant within one symbol transmission. Additional variations of the channel can be caused by motion of surrounding objects (trucks, buses, etc.).

The multipath propagation channel in mobile systems can be presented as a linear filter with a time variant impulse response [8]. The lowpass characterization of the channel is used to do the channel description. Complex lowpass impulse response $h_b(t, \tau)$ [5] describes the channel properties in both delay and Doppler domains in a full way: *t* represents the time variations of the channel due to motion, and τ represents the multipath delays for a fixed time. Physically this function can be interpreted as the response of the channel at time *t* to a unit impulse τ seconds in past.

For systems with a finite bandwidth, impulses separated by a time interval smaller than the time resolution of system $\Delta\tau$ (inverse to the system bandwidth) are received as one impulse, so the impulse response can be presented as the sum of Dirac delta impulses for different excess delays [8]:

$$h_b(t,\tau) = \sum_{i=0}^{N} a_i(t) \cdot e^{-j\Phi_i(t)} \cdot \delta(t - \tau_i(t)) \tag{2.2}$$

where:

N - number of multipath components

α_i - amplitude of i-th component

Φ_i - phase shift of i-th component

$\tau_i = i \cdot \Delta\tau$ - delay of i-th component

$\Delta\tau \leq \frac{1}{B_x}$ - time resolution of the system

B_x - bandwidth of the system

The channel impulse response depends not only on environment properties and system bandwidth, but also on the types of the transmitter and the receiver antennas that are used. Using directional antennas some multipath components can be eliminated from the received signal. Considering the received antenna pattern, the impulse response of the channel can be written as[9]:

$$h_b(t,\tau) = \sum_{i=0}^{N} a_i(t) \cdot e^{-j\Phi_i(t)} \cdot \delta(t - \tau_i(t)) E_r(\theta_i) \tag{2.3}$$

where:

$E_r(\theta_i)$ - value of the receiver antenna pattern for the direction of i-th incoming component

Fig.2.3 presents an example of the discrete time variant impulse response of the channel. When surrounding objects are static, the *t* axis can be described as the mobile station, MS position or as the distance between the BS and the MS.

From the impulse response of the mobile propagation channel one can calculate parameters describing the channel in delay and Doppler domains. The multipath propagation limits the maximum system bandwidth, for which time dispersion of the received signal can be neglected and use of an equalizer is not necessary. Doppler spread determines the speed of the channel changes and limits a maximum symbol duration (a minimum signal bandwidth).

Figure 2.3 The time varing discrete-time impulse response of the multipath channel (extracted from [5])

2.1.2 Time dispersion

In delay domain the spatial average of $\left|h_b(t,\tau)\right|^2$ over a local area is called power delay profile and represents a relative received power as a function of excess delay, when the transmitted signal is one pulse [5]. Usually it is assumed that the first component, the line of sight (LOS) one, arrives at the receiver in delay $\tau = 0$. Examples of power delay profile are presented in Fig. 2.4.

Many useful parameters, describing the time dispersive nature of the propagation channel are derived from measured or simulated power delay profiles [5],[10]:

1. mean excess delay -first moment of delay the profile (the power weighted average of the excess delay)

$$\bar{\tau} = \frac{\int_0^\infty \tau P(\tau)\, d\tau}{\int_0^\infty P(\tau)\, d\tau} \qquad (2.4)$$

2. delay spread - square root of the second central moment of the delay profile (the power weighted standard deviation of the excess delay)

$$\sigma_\tau = \sqrt{\overline{\tau^2} - \bar{\tau}^2} \qquad (2.5)$$

where:

$$\overline{\tau^2} = \frac{\int_0^\infty \tau^2 P(\tau)\,d\tau}{\int_0^\infty P(\tau)\,d\tau} \qquad (2.6)$$

3. maximum excess delay (P dB) - time interval between first and last crossing by the power delay profile of the threshold P dB below the maximum; in Fig.2.4a) it is

$$I_p = (\tau_3 - \tau_1) \qquad (2.7)$$

4. fixed and sliding delay window (q%) - the length of the middle (for fixed window) or the shortest (for sliding window) portion of the power delay profile containing a certain portion of total energy of this profile; in Fig.2.4a) it is

$$W_q = \tau_4 - \tau_2 \qquad (2.8)$$

where:

τ_2 and τ_4 are defined in a way that energy outside the window is split into two equal parts.

a)

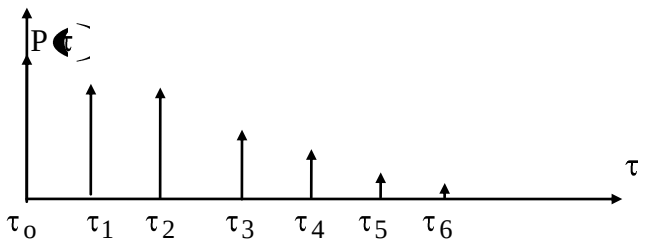

b)

Figure 2.4 Power delay profile for system with a)infinite bandwidth (extracted from [10]) and b) finite bandwidth

These parameters allow to determine how well a digital radio system will work in this multipath environment. For a given modulation method, BER can be calculate as a function of delay spread (with the assumption that an equalizer is not used at the receiver). For example for GMSK modulation the BER is approximately bellow 10^{-3} if the delay spread excess is one tenth of the symbol interval [11]. When the excess delay is greater than the signal duration, intersymbol interferences in the received signal occur and usage of the equalizer is need. Just the sliding delay window parameter determines the necessary equalizer depth to make the receiver work properly.

Besides these parameters in the time domain, it is defined the coherence bandwidth B_c in the frequency domain [8]. Physically, the coherence bandwidth represents the frequency difference between two received signals having strongly correlated amplitudes (amplitude correlation has a certain known value, for example 0.9 or 0.5 - it is dependent on the system and on the technique used for modulation and detection). For frequencies separated more than B_c signals are differently attenuated when they undergo the channel.

Coherence bandwidth determines the dispersive properties of the propagation channel in the frequency domain and is calculated from the delay spread, but there is no exact relation between these parameters, and it is only an estimation. If coherence bandwidth is defined as the bandwidth over which the frequency correlation is above 0.5 then it is approximated by [12]:

$$B_c \approx \frac{1}{2 \cdot \sigma_\tau} \tag{2.9}$$

For signals with a bandwidth B_x smaller than B_c all frequency components of the signal undergo the channel with approximately equal attenuation. Delays of multipath components are much smaller than the signal duration. In the light of the receiver all components arrive at the same moment in time (without delay) and the discrete impulse response of the channel contains only one Dirac delta for $\tau = 0$. In frequency domain this corresponds to the channel having constant gain and linear phase for all signal frequencies. Of course the module of this impulse can vary in time because of the receiver motion and changes of surrounding objects, so variation of the received signal can occur.

This type of signal propagation is called flat fading, because the spectrum of the received signal is the same as that of the transmitted one. Fig.2.5 presents this kind of fading in time and frequency domains.

Figure 2.5 Flat fading characteristics in time and frequency domains (extracted from [5])

For signals with a bandwidth compared in value or wider than B_c frequency components of the signal undergo the channel with different attenuations, some components being more attenuated than others. Due to different delays of multipath components, which cannot be neglected, the time duration of the received signal increases, which causes a decrease of the signal bandwidth. When B_x is much larger than B_c time dispersion of the signal is significant, the received signal bandwidth is limited by the propagation channel and it is smaller than that of the transmitted one. The discrete impulse response in this case cannot be simple Dirac delta functions. It must consider the time dispersive nature of the multipath propagation channel, so it is the sum of Dirac deltas for different time delays.

This type of signal propagation is called frequency selective fading, because the spectrum of the received signal is smaller as that of the transmitted one. Fig.2.6 presents this kind of fading in time and frequency domains.

Figure 2.6 Frequency selective fading characteristics in time and frequency domains (extracted from [5]).

2.1.3 Time variation of the channel

To describe the channel properties in the Doppler domain one uses the coherence time, T_c parameters [8], which characterizes the time varying nature of channel. Coherence time is the time duration over which two received signals have a strong correlation of amplitudes, and the channel can be considered as time invariant during these signals transmission. For signals with greater time separation the channel can change during the transmission, and received signal amplitudes will be different.

If coherence time is defined as the time over which the time correlation is above 0.5 it is approximated by [5]:

$$T_c = \frac{9}{16 \cdot \pi \cdot f_m} \tag{2.10}$$

where:

$f_m = \frac{v}{\lambda}$ - maximum Doppler shift

Another common approximation for T_c is (specially for digital communication systems) [5]:

$$T_c = \frac{0.423}{f_m} \tag{2.11}$$

For a signal with symbol duration smaller than T_c the channel can be considered as static over one or several symbols duration and distortion does not occur. In this case the frequency bandwidth of the signal is much greater than the Doppler shift and frequency dispersion is not observable. This type of signal propagation is called time flat fading or slow fading. This occurs if:

$$T_x << T_c \quad \text{and} \quad \mathrm{B_x} >> f_m \tag{2.12}$$

If the signal duration is greater than T_c the channel changes over one symbol duration and the received symbol is distorted. The frequency bandwidth of the signal is smaller than Doppler shift and frequency dispersion can be observed. This distortion is called time selective fading or fast fading. This occurs if:

$$T_x > T_c \quad \text{and} \quad \mathrm{B_x} < f_m \tag{2.13}$$

The fast and the slow fadings are determined only by the rate of changes of the propagation channel in time (depends on the velocity of the mobile or surrounding objects).

2.2 Modeling of the multipath propagation channel

In order to properly design a mobile communication system the knowledge of the mobile multipath propagation channel models is necessary. This allows to choose in a design phase proper modulation and error correction schemes for the system. A short description of the channel modeling methods is presented next. In general these methods can be divided on:

1. statistical - based on measurements or on statistical scattering models of the signal propagation in a multipath environment, and give statistical distributions of the received signal parameters described only by small amount of variables.
2. deterministic - based on equations describing the signal propagation, they require exact a description of the propagation scenario (objects positions and orientations, their electrical properties) and are complicated to implement.

The scattering models describing the signal propagation in the multipath environment assume that the signal in every receiving point is the result of *N* different path waves. Each of multipath waves is characterized by amplitude, phase shift and spatial angles of arrival (in the horizontal and vertical planes), which are all random and statistically independent [10]. Other assumptions are that [7]:

1. the transmission channel is sufficiently random, can be described as a wide sense stationary uncorrelated channel, WSSUS, which mean that the signal variation for different delays is uncorrected and correlation properties of the channel are stationary (invariant under translation in time and frequency);
2. the number of multipath components is sufficiently large, enabling the use of the central limit theory

Then the received signal is accurately represented by a complex Gaussian process. From this process, statistics describing the signal properties can be calculated: complex envelope of the signal, level crossing rate, average duration of fades and spatial correlations between signals [13]. Exact description of scattering models are presented in literature: Clarke's model [14], assumes that the received signal is the sum of horizontally traveled scattering waves (without direct wave), the phase and horizontal angle of arrival (assumed apriori, it determines spatial correlation properties of the model) having uniform probability in the interval $[0, 2\pi]$; three dimensional extension of this model is presented in [10].

The most useful statistic, allowing to model the impulse response of the propagation channel, is the complex envelope distribution of the received signal. For the narrowband signals it is modeled like a Rayleigh or Rician distribution.

Rayleigh distribution is used to describe the statistical time varying nature of the signal envelope when LOS between the transmitter and the receiver does not exist (only multipath components are received). The probability density function, (PDF) of the signal envelope for this distribution, presented on the Fig.2.7, depends on only one parameter, σ^2 [5]:

$$p(r) = \begin{cases} \frac{r}{\sigma^2} \exp\left(-\frac{r^2}{2\sigma^2}\right) & (0 \le r \le \infty) \\ 0 & (r < 0) \end{cases} \tag{2.14}$$

where:

r - signal envelope amplitude

σ^2 - mean power

$\frac{r^2}{2}$ - short-term signal power

The probability that the envelope of the received signal does not exceed a specific value R is given by the cumulative distribution function (CDF):

$$P(R) = \Pr(r < R) = \int_0^R p(r)dr = 1 - \exp\left(-\frac{R^2}{2\sigma^2}\right) \tag{2.15}$$

Figure 2.7 Probability density function of the Rayleigh distribution (extracted from [10])

Standard parameters calculated for this distribution are:

- mean value

$$r_{mean} = E\{r\} = \int_0^\infty rp(r)dr = \sigma\sqrt{\frac{\pi}{2}} = 1{,}2533\sigma \tag{2.16}$$

- variance of the envelope which represents the ac power of the signal

$$\sigma_r^2 = E\{r^2\} - E\{r\}^2 = \sigma^2\left(\frac{4-\pi}{2}\right) = 0{,}4292\sigma^2 \qquad (2.17)$$

- median value

$$r_M = \sqrt{2\sigma^2 \ln 2} = 1.1774\sigma \qquad (2.18)$$

Rician distribution is used to describe the statistical time varying nature of the signal envelope when LOS between the transmitter and the receiver exists (or other dominant stationary component). At the output of an envelope detector this has the effect of adding a dc component to the random multipath. The PDF of the signal envelope for this distribution is [5]:

$$p(r) = \begin{cases} \frac{r}{\sigma^2}\exp\left(\frac{r^2+r_s^2}{2\sigma^2}\right) I_o\left(\frac{rr_s}{\sigma^2}\right) & (0 \le r \le \infty) \\ 0 & (r < 0) \end{cases} \qquad (2.19)$$

where:

r - signal envelope amplitude

r_s - peak amplitude of the dominant signal

$I_o(\cdot)$ - the modified Bessel function of the first kind and zero-order

σ^2 - mean power of the multipath components

This distribution function is often described in term of a parameter *K*, which is defined as the ratio between the deterministic signal power and the variance of the multipath:

$$K = \frac{r_s^2}{\sigma^2} \qquad (2.20)$$

Figure 2.8 Probability density function of the Rician distribution: a) $K = -\infty$ dB (Rayleigh); b) $K = 6$ dB; c) $K >> 1$ dB (extracted from [10]).

If K goes to zero (the amplitude of the dominant path decreases), the Rician distribution degenerates in a Rayleigh distribution, whilst if $K >> 1$, the distribution becomes a Gaussian distribution with a mean value r_s. The PDF of the Rician distribution is presented in Fig.2.8.

For wideband channels the statistical models base on (2.2) and can be presented as a taped-delay line, Fig.2.9 [8]. Each delayed component is modeled as a large number of waves arriving at the same time from different directions (like in narrowband channels) [7], and a description based on Rician (direct wave) and Rayleigh (multipath waves) distributions can be used. The delay $\Delta\tau$ depends on the system bandwidth.

Figure 2.9 Taped-delay line - model of the channel impulse response (extracted from [8])

The real mobile propagation channel is in many cases non stationary and to use simple mathematical models the channel is introduced as stationary for restricted time T and frequency B intervals, Quasi-WSSUS channel [8]. For times or frequencies larger than T or B correlation functions cannot be assumed invariant. The channel is analyzed in small time or spatial intervals as stationary and then the large scale properties of it are obtained by examining the small scale statistics over a larger area; in this case the parameters of the models change in time. That is modeled by considering Doppler spread of each impulse response [16], or by considering that contains N states and choosing one of them is a random process [17]. Extraction of statistical models parameters, describing the signal envelope, are presented in [15] for narrowband channels with existing LOS path (Rician fading) and in [16], [17] for wideband channels.

Deterministic modeling of the propagation channel is based on equations describing the signal propagation. An exact analysis can be done by solving Maxwell's equations with

boundary conditions representing the physical properties and geometry of the surrounding environment, but this is possible only for the simplest scenarios. A simpler analytical approach, commonly used, is the assumption that radio waves propagate as light (ray propagation) [7]. Under this condition the received signal is the sum of:

1. reflected rays, which can be described by Geometrical Optics method [18] using Snell's reflection law to determine the path of a ray and reflection coefficient to determine amplitude of each ray
2. diffracted rays on sharp edges of objects with dimensions similar to the wavelength, which can be describe by diffraction theory, for example Uniform Theory of Diffraction, UTD [19]

For very high frequencies the wavelength is much smaller than the scenario objects dimensions, thus a model can take into account reflections only.

Deterministic models of the propagation channel in comparison with statistical ones, described by few parameters, require many complicated calculation (fast computers must be used) and exact knowledge of the environment (positions, orientations, electrical properties, roughness of the objects; BS and MS position etc..). Nevertheless they allow to determine the received signal in specific conditions, for example what changes occur when directional antennas are used or when the receiver changes its position.

2.3 Propagation channel at the 60 GHz band

2.3.1 Signal attenuation

At high frequencies signals are additionally attenuated by oxygen, water vapour and rain, Fig.2.10 [11].

Figure 2.10 Oxygen absorption and rain attenuation (extracted from [21],[22])

These effects are negligible at the UHF band, but at higher frequencies they must be considered. In 60 GHz band there is a peak of oxygen absorption. which causes a large signal attenuation, about 15 dB/km [21].

The attenuation for a path *d*[km] is given by

$$L_o\,[dB] = \gamma_o \cdot d \tag{2.21}$$

where:

d - distance in km

γ_o - the attenuation coefficient for oxygen absorption, at the [60,66] GHz band one has [20]:

$$\gamma_o\,[dB/km] = \begin{cases} 15.10 - 0.104\cdot(f-60)^{3.26} & \text{for } 60\text{ GHz} \le f \le 63\text{ GHz} \\ 11.35 + (f-63)^{3.25} - 5.53\cdot(f-63)^{1.27} & \text{for } 63\text{ GHz} \le f \le 66\text{ GHz} \end{cases} \tag{2.22}$$

where:

f is in GHz

In this particular of [60,66] GHz band the oxygen attenuation decreases when the frequency increases (inversely to the behavior of the UHF band). So this fact should be taken into account when frequencies will be chosen for the up and down transmission links.

The water vapour absorption can be neglected at these frequencies [11], because it is much smaller than oxygen absorption (about 0.2 dB/km).

The rain attenuation coefficient is proportional to the fall rate *R* [21], and for a very intense rain it can be higher than the oxygen one.

$$\gamma_r\,[dB/km](f,R) = k(f)R^{a(f)} \tag{2.23}$$

where:

γ_r - rain attenuation coefficient

R - fall rate

k and *a* - constants depended on the wave polarization.

For 60 GHz band these variables are described by following expression [20]:

$$k(f) = \begin{cases} 10^{1.296 \cdot \log(f) - 2.497} & \text{V polarisation} \\ 10^{1.203 \cdot \log(f) - 2.290} & \text{H polarisation} \end{cases} \quad (2.24)$$

$$a(f) = \begin{cases} 1.647 - 0.463 \cdot \log(f) & \text{V polarisation} \\ 1.703 - 0.493 \cdot \log(f) & \text{H polarisation} \end{cases} \quad (2.25)$$

where:

f is in GHz

Attenuation of signal caused by fog, snow, sleet and others can be neglected because their attenuation coefficients are small and they occur with a very low probability [20].

The average received power depends on the distance between the transmitter and the receiver and on attenuation by oxygen and rain [20]:

$$P_r[\text{dBm}] = -32{,}4 - 30\alpha + P_t[\text{dBm}] + G_t[\text{dBi}] + G_r[\text{dBi}] - 10\alpha \log(d[\text{km}]) - 20\log(f[\text{GHz}]) - \gamma_o[\text{dB/km}] \cdot d[\text{km}] - \gamma_r[\text{dB/km}] \cdot d[\text{km}] \quad (2.26)$$

where:

P_r - received power

P_t - transmitted power

G_r - receiver antenna gain

G_t - transmitter antenna gain

d - distance between the transmitter and the receiver

f - signal frequency

α - is from range $\langle 2;2{,}4 \rangle$

For small distances between the receiver and the transmitter the signal propagation is similar to a free space propagation

2.3.2 Model for the signal propagation

In MBS, cells will be small (typical a few hundreds meters) and LOS between the BS and the MS must exist. The wavelength (about 5mm) is very small in comparison with the dimensions of the surrounding objects and the geometrical optics approach (only reflections) is used to obtain the propagation model [23]. The received signal is the sum of the direct ray with many reflected ones (one and multiple reflections). Each of these rays has different delays, depending on the distance between the transmitter and the receiver and surrounding objects scenario, different amplitudes and phase shifts, which depend on following factors:

1. transmitted field (magnitude and polarization)
2. transmitter and receiver antennas gain and radiation pattern
3. path length
4. reflection coefficient of the surfaces
5. oxygen and rain attenuation

The electrical field around the receiver antenna is sum of the direct ray field with the fields of reflected rays[23]:

$$E(t) = E_d(t - \tau_d(t)) + \sum_{i=1}^{N} E_{ri}(t - \tau_i(t)) \tag{2.27}$$

The assumption that all surrounding objects in the scenario are static and only the MS is moving is done, thus the dependence of parameters in (2.27) on time is caused only by the receiver position:

$$E(t, r) = E_d(t - \tau_d(r)) + \sum_{i=1}^{N} E_{ri}(t - \tau_i(r)) \tag{2.28}$$

where:

r - distance between BS and MS

The amplitude of each reflected ray is determined by reflections on objects' surfaces. It is impossible to give a exact description of the reflecting objects at the wavelength scale, so a statistical description by standard roughness deviation of these objects is used. In this case reflections depend not only on the electric properties of surface (relative dielectric constant and loss tangent) but also on its roughness (the non flat surface causes non-coherent reflection). For the small roughness case the reflection coefficient is [10]:

$$\Gamma^{G} = \Gamma \cdot e^{\frac{\gamma^2}{2}} \tag{2.29}$$

where:

Γ - the Fresnel reflection coefficient

γ - parameter associated to the Rayleigh criterion of roughness

A surface can be considered as smooth if $\gamma < 0.3$:

$$\gamma = 4 \cdot \pi \frac{\sigma_h}{\lambda} \cdot \sin(\theta) \tag{2.30}$$

where:

σ_h - surface height standard deviation

θ - incidence angle (measured to the surface tangent plane)

λ - wavelength

The Fresnel reflection coefficient is [5]:

$$\Gamma(\theta,\varepsilon)=\begin{cases}\dfrac{\sin\theta-\sqrt{\varepsilon_r-\cos^2\theta}}{\sin\theta+\sqrt{\varepsilon_r-\cos^2\theta}} & \text{for } \perp \text{ polaristion}\\ \dfrac{\varepsilon_r\sin\theta-\sqrt{\varepsilon_r-\cos^2\theta}}{\varepsilon_r\sin\theta+\sqrt{\varepsilon_r-\cos^2\theta}} & \text{for } \| \text{ polaristion}\end{cases} \qquad (2.31)$$

where:

$\varepsilon_r=\varepsilon_r'-j\varepsilon_r'\cdot\tan\delta$ -complex relative dielectric constant

ε_r' - the relative dielectric constant

$\tan\delta$ - loss tangent

Due to different reflection coefficient for waves with orthogonal polarization, depolarization of signal can occur.

Each multipath component of the electrical field produces in the receiver a signal which depends on the receiver antenna gain in the direction of the incoming component, so using directional antennas it is possible to minimize the number of multipath components which are received, in this case the delay spread of the channel decreases. But there is a problem when the antenna is not pointed towards the transmitter, since in this case communication can be lost.

The signal produced by each incoming wave is given by:

$$V_i=E_i\cdot h_i \qquad (2.32)$$

where:

h_i - effective antenna height, in a direction of the i-th incoming component

E_i - electric field amplitude of the i-th component

Due to the finite bandwidth of the receiver, all signals which are received in a time interval smaller than the time resolution of the system are represented in the receiver as a single signal. For the system with a bandwidth of 200 MHz (MBS) the time resolution is 5 ns and all rays arrived at the receiver in the same 5 ns beam are received as one ray which is characterized by its delay τ_b. One can write the receiver signal in one beam as:

$$V_b=\sum_{bi=0}^{Nb}V_{bi} \qquad (2.33)$$

where:

Nb - number of rays within one delay beam

The power in each delay beam is given by:

$$P_b = \frac{\lambda^2 |V_b|^2}{8 \cdot \pi \cdot Z} \tag{2.34}$$

where:

Z - free space characteristic impedance

λ- wavelength

The power delay profile of the received signal and total received power for each position is:

$$P(t, \vec{r}) = \sum_{b=1}^{N} P_b(t - \tau_b(\vec{r})) \tag{2.35}$$

$$P(\vec{r}) = \int_0^{\infty} P(t, \vec{r})\, dt \cong \sum_{b=1}^{Nb} P_b(\tau_b(\vec{r})) \tag{2.36}$$

This approach, considering a discrete description of time, has some errors associated to it.

3. Analysis of results from simulations

3.1 Simulation scenario

The simulations have been done by using a programme based on the deterministic geometrical optics model, described in the previous last section, with additional assumptions [18]:

1. Rain attenuation is not considered
2. Only reflected rays up to third order are considered. This is because higher order reflected rays are strongly attenuated, and different orientations of buildings in a real scenario produce more rays with one and two reflections; the importance of high order reflected rays is much smaller then [23].

The simulation scenario, was taken as the typical for MBS: a street with walls on both sides, is presented in Fig.3.1. Ground and walls are described by their electrical parameters (dielectric constant and conductivity) and by the standard deviation of their roughness. It is possible to simulate discontinuous properties of these surfaces, which allows to model different buildings materials, crossings etc. The BS and the MS positions are described by their distances from the wall and by the antennas heights. The BS is fixed (typically placed on a lamp) and the MS moves along the street parallel to the walls. Radiation patterns and orientations of the antennas have been taken account.

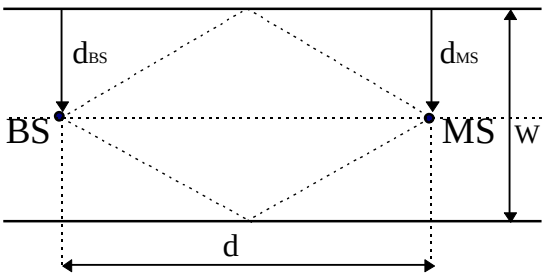

Figure 3.1 Simulation scenario

The following rays reach the receiver (with the assumption that the BS antenna is higher than the MS one) [11]:

- one direct ray
- three first order reflected rays (two walls reflections and one ground reflection)

- four second order reflected rays (two wall-wall reflections, two ground-wall reflections)
- six third order reflected rays (two wall-wall-wall reflections, two wall-wall-ground reflections, two wall-ground-wall reflections)

This signal propagation model has been verified by comparison of its results with measurement data for the same propagation scenarios [23].

The programme used in the simulations, calculates discrete power delay profiles (considering system bandwidth) for each position (at a given step) of the receiver along the street. Using these results the average discrete power delay profile of the street has been calculated by averaging the power in the same delay beam for different positions of the receiver. Then, from this profile, mean delay $\bar{\tau}$ and delay spread σ_τ have been calculated using the following formulas:

$$\bar{\tau} = \frac{\sum_{i=0}^{N} P_i \tau_i}{\sum_{i=0}^{N} P_i} \tag{3.1}$$

$$\sigma_\sigma = \sqrt{\overline{\tau^2} - \bar{\tau}^2} \tag{3.2}$$

$$\overline{\tau^2} = \frac{\sum_{i=0}^{N} P_i \tau_i^2}{\sum_{i=0}^{N} P_i} \tag{3.3}$$

where:

P_i - relative power received in i-th beam

τ_i - delay of the i-th beam

N - number of beams in the average power delay profile

The standard street corresponding to a typical propagation scenario in a MBS cell has been defined and used in simulations. It has been described as:

- concrete ground and walls with $\varepsilon_r = 6{,}14$ and $\tan\delta = 0{,}0491$, with roughness $\sigma_h = 1\text{mm}$
- street width $W = 10\text{m}$
- street length $L = 200\text{m}$
- BS position $d_{BS} = 5\text{m}$ and height $h_{BS} = 5\text{m}$
- MS position $d_{MS} = 3{,}5\text{m}$ and height $h_{MS} = 1{,}8\text{m}$

- both antennas isotropic
- system bandwidth $B_x = 200\text{MHz}$

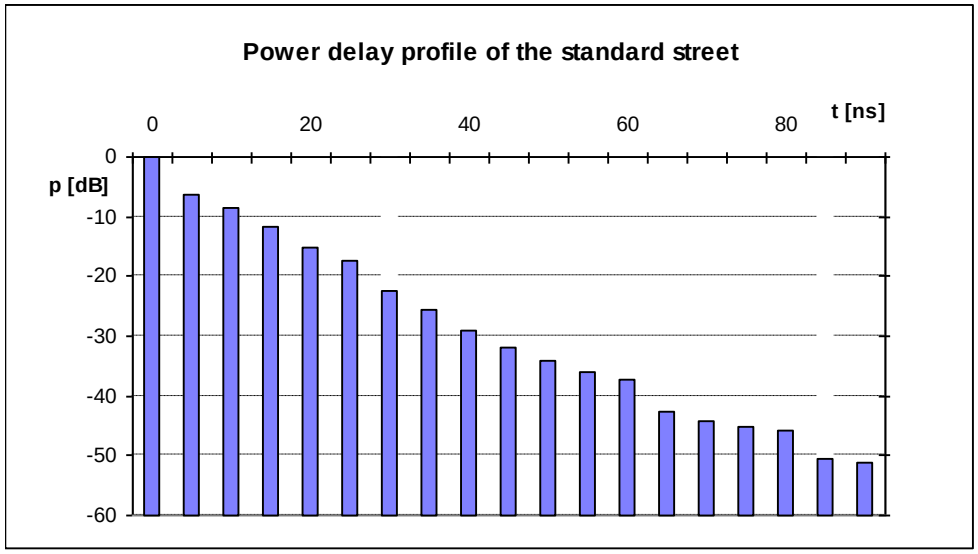

Figure 3.2 Discrete delay profile of the standard street.

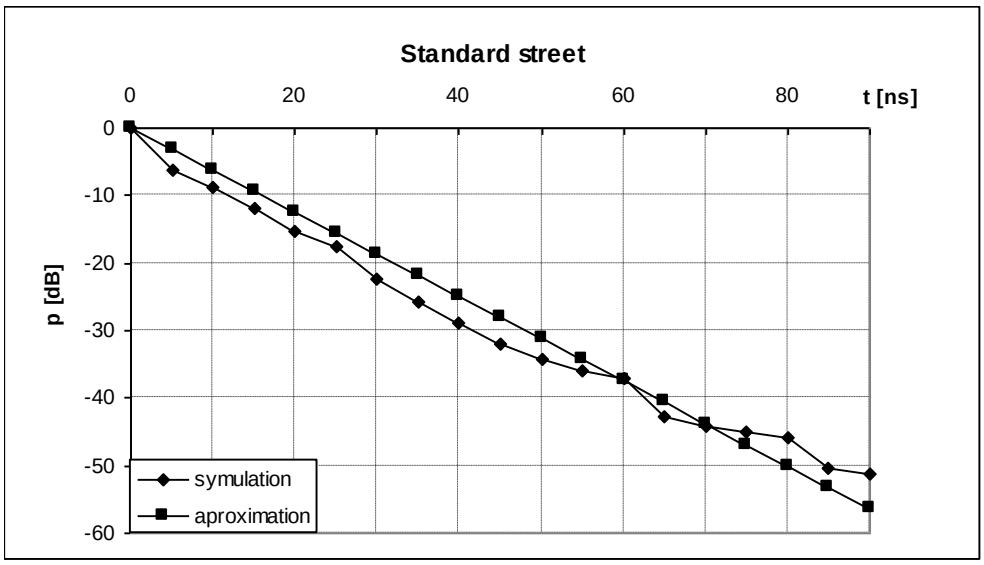

Figure 3.3 Continuous power delay profile for the standard street and its exponential approxymation

The discrete power delay profile of the standard street is presented in Fig.3.2, and its envelope (continuous extension for infinite system bandwidth) in Fig.3.3. The envelope of the profile is a decreasing function of the delay: the large delay components of the profile are produced by multiple reflected rays, so that their amplitudes are smaller in comparison to the direct ray,

due to reflection and higher attenuation (longer path length). The components with the larger delays are received for small distances between the transmitter and the receiver (larger length differences between reflected and the direct rays), Fig.3.4. Amplitudes of these components depend mainly on reflecting surfaces properties. When the distance between BS and MS increases the path length differences between these rays and the direct ray is smaller and the received signal contains only components with small delays, so in this case the propagation channel is less dispersive.

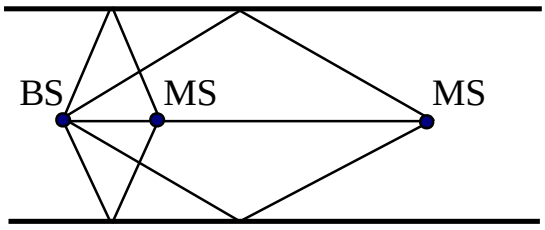

Figure 3.4 Ilustration of path length difference between LOS and wall reflected rays for a small and a large distance between the BS and the MS

The profile can be approximated with good accuracy (mean square error lower than 1 dB) by an exponential function (linear in logarithmic scale):

$$p(\tau) = e^{-m\tau} \tag{3.4}$$

where:

m - slope of power delay profile in logarithmic scale

For this approximation parameters $\bar{\tau}$ and σ_τ can be calculated in an analytical way, and they have the same value:

$$\sigma_{\tau\,\text{analit}} = \bar{\tau}_{\text{analit}} = \frac{1}{m} \tag{3.5}$$

This value corresponds to an infinite bandwidth of the receiver. Tab.3.1 presents the parameters calculated from the different profiles, obtained from simulations, their exponential approximation, using (3.1) and (3.2) and the analytical value from (3.5). The parameters τ_{approx} and σ_{approx} have larger value than parameters τ and σ. It is caused by small differences between obtained profile and its approximation (for small delays, (components with high amplitudes) the approximating function is above the obtained profile). These parameters are a function of the system bandwidth and are different from the analytical value. But τ_{approx} and σ_{approx} are similar to this value. Delay spread σ_{approx} is smaller about 2%

from σ_{analit} difference for mean delays is larger (because (3.2) converges faster than (3.3) to their boundary given by (3.5)); in the results to follow the analytical value of mean delay and delay spread is omitted.

Mean deay [ns]			Delay spread [ns]		
simul. prof. τ	approx. prof. τ_approx	analitycal τ_analityc	symul. prof. σ	approx. prof. σ_approx	analitycal σ_analityc
3,33	4,75	6,95	6,14	6,80	6,95

Table 3.1 Delay parameters for the standard street

Simulations for different street scenarios and system parameters have been done in order to determine their influence on the time dispersive properties of the propagation channel (caused by multipath propagation of the signal). The defined standard street scenario has been used in these simulations, considering different values for one parameter and keeping the others constants. the following parameters have been considered:

1. system bandwidth
2. walls materials (electric properties and roughness)
3. width and length of the street
4. position of the BS and the MS (distance from the wall) in the street
5. antennas height
6. type of antennas

Results from these simulations are presented in next sections of this chapter. The approximating delay profile has been used to characterize the profile for different conditions.

3.2 Dependence on system bandwidth

Simulations have been done for values of the system bandwidth ranging form 20 MHz to 1 GHz. When the system bandwidth increases the time resolution of the system decreases and the discrete power delay profile contains more delayed components, Fig.3.5. However the envelopes of these profiles are independent of the system bandwidth (in the limit when $B_X \to \infty$, the discrete power delay profile tends to its continuous approximation). Profiles for different system bandwidth are presented in Fig.3.6. The difference for $B_X = 20$ MHz (time

resolution 50 ns) is because the discrete profile in this case has only two components: the direct one and one delayed, so small errors of these components powers lead to large changes on the approximating profile slope.

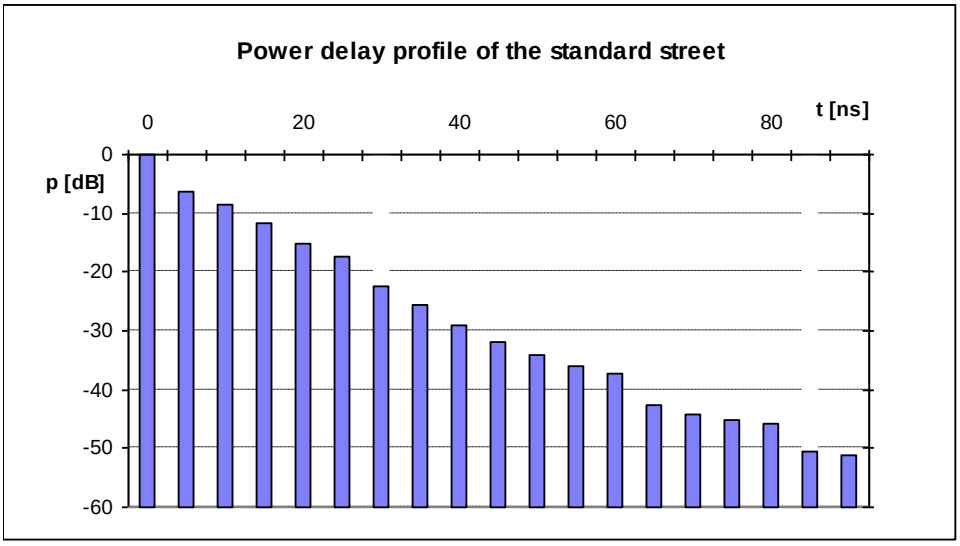

a)

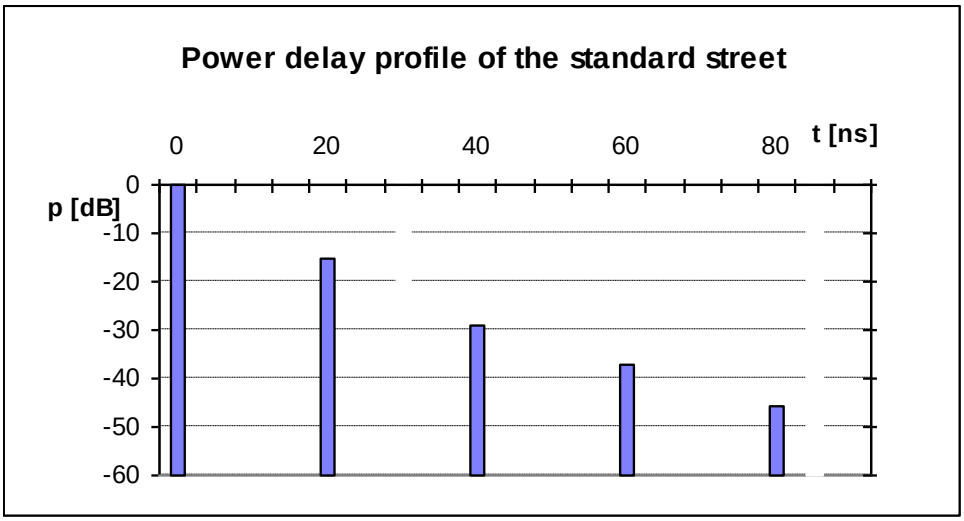

b)

Figure 3.5 Discrete power delay profile for different system bandwidths: a) 200 MHz; b) 50 MHz

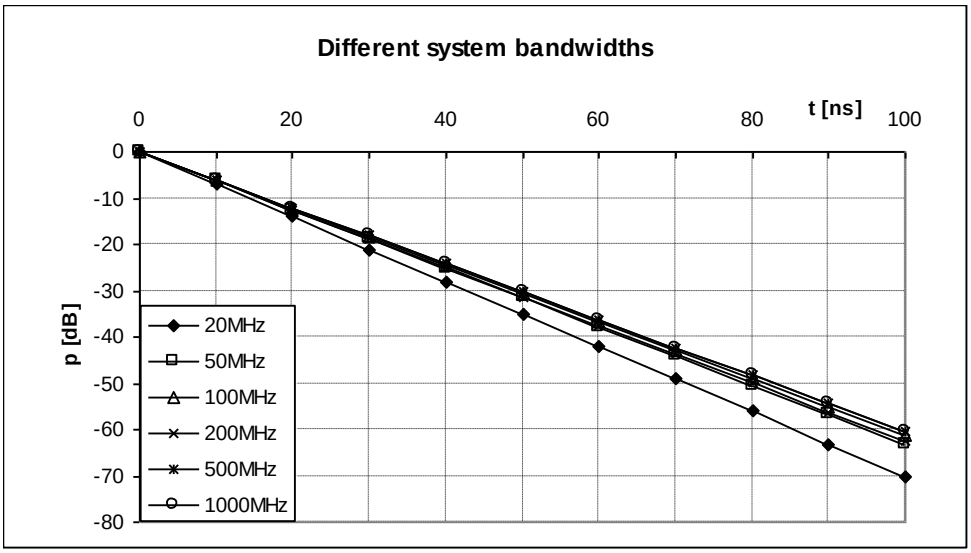

Figure 3.6 Power delay profiles for different system bandwidths

Bx [MHz]	Mean deay [ns]			Delay spread [ns]		
	simul. prof. τ	approx. prof. τ_approx	analitycal τ_analityc	symul. prof. σ	approx. prof. σ_approx	analitycal σ_analityc
20	0,02	0,02	6,20	0,88	0,88	6,20
50	0,59	1,16	6,88	3,54	4,95	6,88
100	2,10	3,24	7,10	5,30	6,55	7,10
200	3,33	4,75	6,95	6,14	6,80	6,95
500	5,65	6,24	7,19	7,25	7,17	7,19
1000	6,82	6,71	7,19	7,48	7,19	7,19

Table 3.2 Delay parameters for different system bandwidths

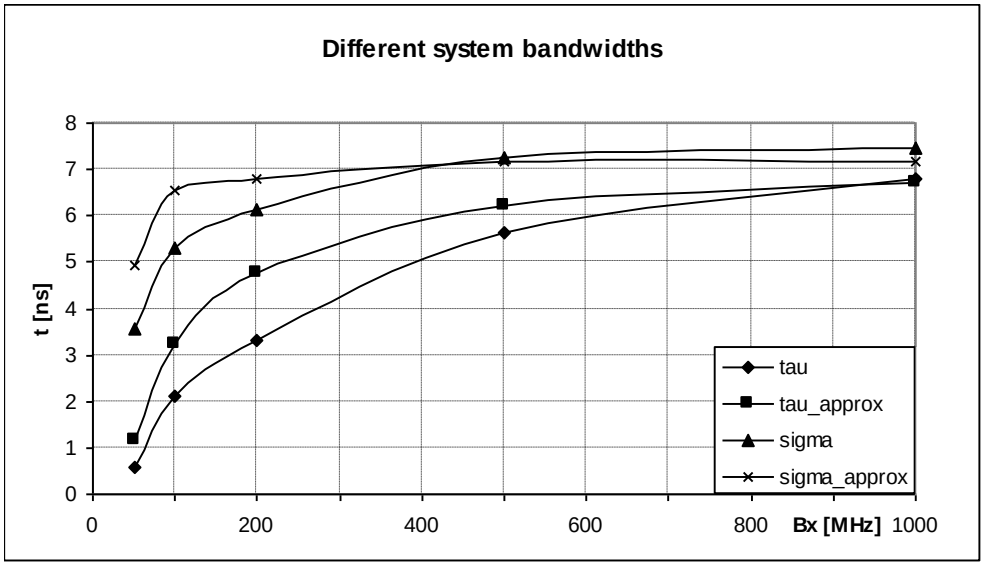

Figure 3.7 Delay parameters as a function of system bandwidth

The delay parameters are presented in Tab.3.2 and in Fig.3.7. Their values are a function of the system bandwidth and increase from 0,1 ns for $B_X = 20\,\text{MHz}$ to above 7 ns for $B_X = 1\,\text{GHz}$, but for large bandwidths these changes are smaller (parameters seek to their boundary, for τ_{approx} and σ_{approx} it is analytical value presented in table, for $B_x > 200\,\text{MHz}$ delay spread is very similar to this value). For larger system bandwidth differences between parameters calculated from simulated profile and from its approximation are smaller.

Dependence of the delay parameters on the system bandwidth can be approximated (for values of B_x considered in simulations) by the following function:

$$\sigma = a \cdot \tanh(b \cdot B_X) \tag{3.6}$$

where *a* and *b* depend on the street scenario, and σ represents the mean delay or the delay spread. For the delay parameters calculated from simulation profile the approximation is:

$$\tau = 7 \tanh(0{,}0024 \cdot B_x) \tag{3.7}$$

$$\sigma = 7{,}7 \tanh(0{,}0055 \cdot B_x) \tag{3.8}$$

where:

mean delay τ and delay spread σ are in ns

B_X - system bandwidth in MHz

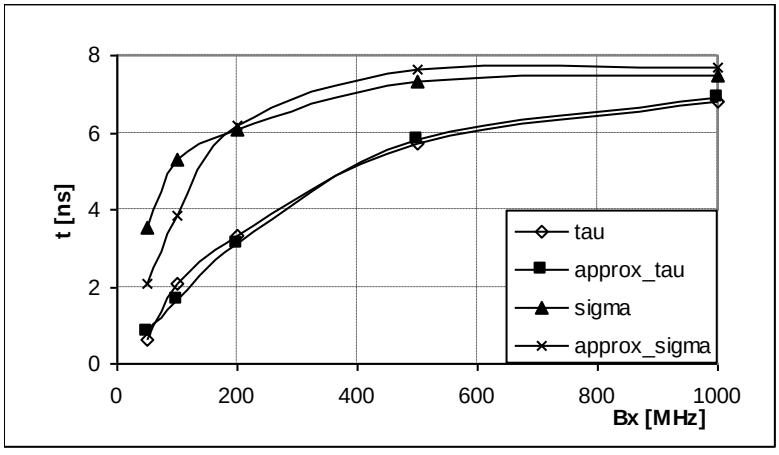

Figure 3.8 Approximation of delay parameters by hiperbolic tangents function of system bandwidth

Results of these approximation are presented in Fig.3.8. Some differences are observed for the delay spread for small B_X, where the approximation gives smaller values for this parameters; for the mean delay this approximation is very good.

3.3 Dependence on walls materials

Simulations have been done for different walls materials, electrical parameters of the materials being taken from [11]. Electric parameters of walls and ground determine reflection of rays from these surfaces. Results are presented in Fig.3.9 and in Table 3.3. Reflected rays have larger amplitude for materials with larger ε_r and $\tan\delta$, but the dielectric constant has a larger influence. For example, aerated concrete in comparison with acrylic glass has almost a four times larger loss tangent and only slightly smaller dielectric constant, but for it better channel characteristics (larger slope of the power delay profile) than for acrylic glass are obtained.

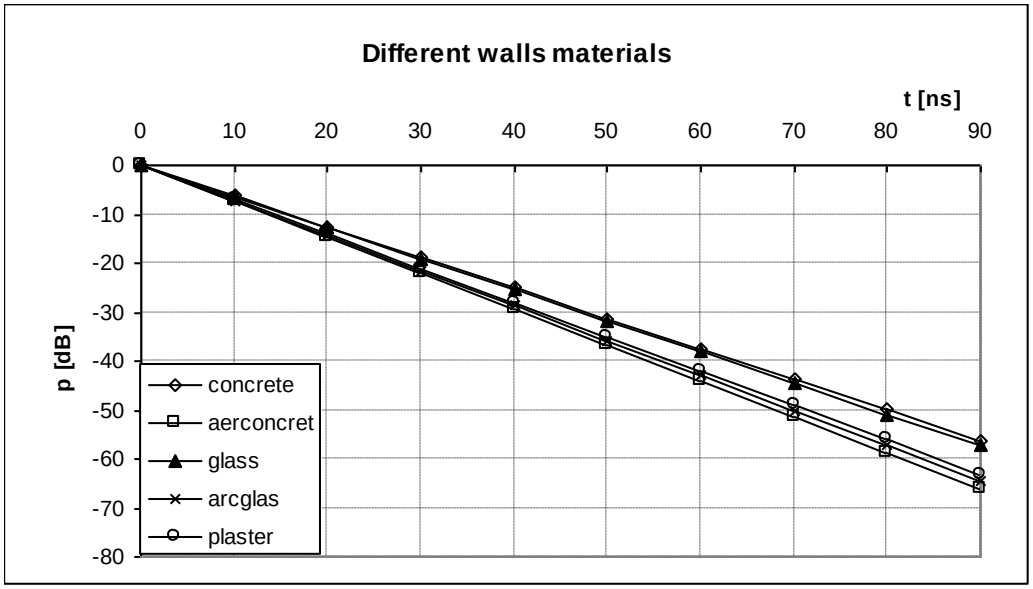

Figure 3.9 Power delay profiles for different walls materials

BS-MS antennas	electrical properties of material		Mean deay [ns]		Delay spread [ns]	
	ε_r	$\tan\delta$	simul. prof. τ	approx. prof. τ_approx	symul. prof. σ	approx. prof. σ_approx
concrete	6,14	0,0491	3,33	4,75	6,14	6,80
aerated concrete	2,26	0,0449	2,06	3,76	4,59	5,74
glass	5,29	0,0480	3,17	4,63	5,96	6,68
acrylic glass	2,53	0,0119	2,23	3,90	4,82	5,89
plasterboard	2,81	0,0164	2,39	4,03	5,02	6,03
stone	6,81	0,0401	3,44	4,82	6,25	6,88

Table 3.3 Delay parameters for different walls materials

Delay parameters are presented in Tab.3.3. For the usual materials (typical for buildings) they vary in a small range: [2 , 3,5] ns for mean delay τ and [4,5 , 6,3] ns for delay spread σ. So the electrical properties of walls' materials do not have a great influence on the propagation channel properties.

3.4 Dependence on the roughness of reflecting surfaces

Simulations have been done for the standard street scenario with changes in the walls and ground roughness deviation in the range [0 , 2] mm. The obtained power delay profiles are presented in Fig.3.10. When the roughness of the reflecting surface increases, the reflection coefficient decreases very fast due to noncoherent scattering of the signal, and the slope of the profile increases. So the power delay profile is much more sensitive on the changes of the walls roughness than on the changes of their electrical properties. For a small distance between the receiver and the transmitter amplitudes of the multipath components reflected from flat surfaces can be high, which causes worse properties for the channel. For larger distances these components have smaller delays and, additionally in this case, the dependence of reflected rays amplitudes on reflecting surfaces roughness is smaller (Γ is almost one due to a small incidence angle).

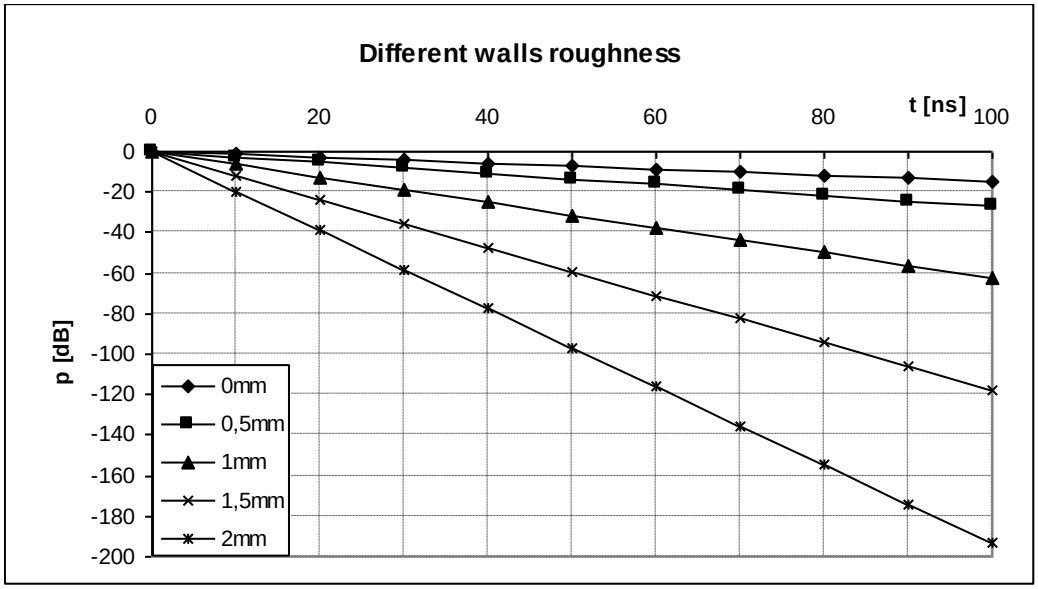

Figure 3.10 Power delay profiles for different roughness of reflecting surfaces

Delay parameters are presented in Tab.3.4. and Fig.3.11. They change in a large range from a fraction of ns for rough reflecting surfaces to more than 20 ns for flat surfaces.

The variation of these parameters for the considered range of the roughness deviation σ_h can be approximated by the exponential function:

$$\sigma = a \cdot e^{-b \cdot \sigma_h} \tag{3.9}$$

where:

a and *b* constants dependent on the street scenario

σ_h [mm]	Mean deay [ns]		Delay spread [ns]	
	simul. prof. τ	approx. prof. τ_approx	symul. prof. σ	approx. prof. σ_approx
0	27,15	23,44	26,03	22,01
0,5	13,05	13,46	17,47	15,24
1	3,33	4,74	6,14	6,80
1,5	1,23	1,73	3,04	3,41
2	0,54	0,61	1,84	1,84

Table 3.4 Delay parameters for different roughness of reflecting surfaces

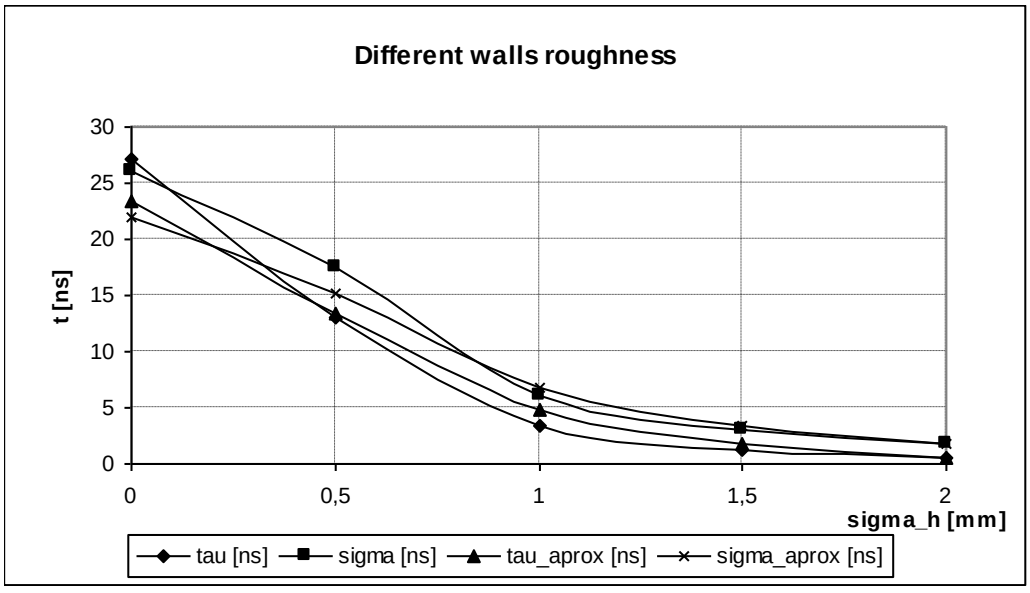

Figure 3.11 Delay parameters for different roughness of reflecting surfaces

For the parameters calculated from simulations results one has:

$$\tau = 27e^{-1,95\sigma_h} \tag{3.10}$$

$$\sigma = 29e^{-1,35\sigma_h} \tag{3.11}$$

where:

$\bar{\tau}$ mean delay and σ_τ delay spread in ns

σ_h - standard roughness deviation in mm

Results of these approximations are presented in Fig.3.12. There are differences between calculated parameters and their approximations for small roughness ($\sigma_h < 1$mm). In this range of roughness better results are obtained with function $e^{-b\cdot\sigma^2_h}$, but the small amount of simulation points does not allow to verify this hypothesis (this function gives worse results for larger σ_h).

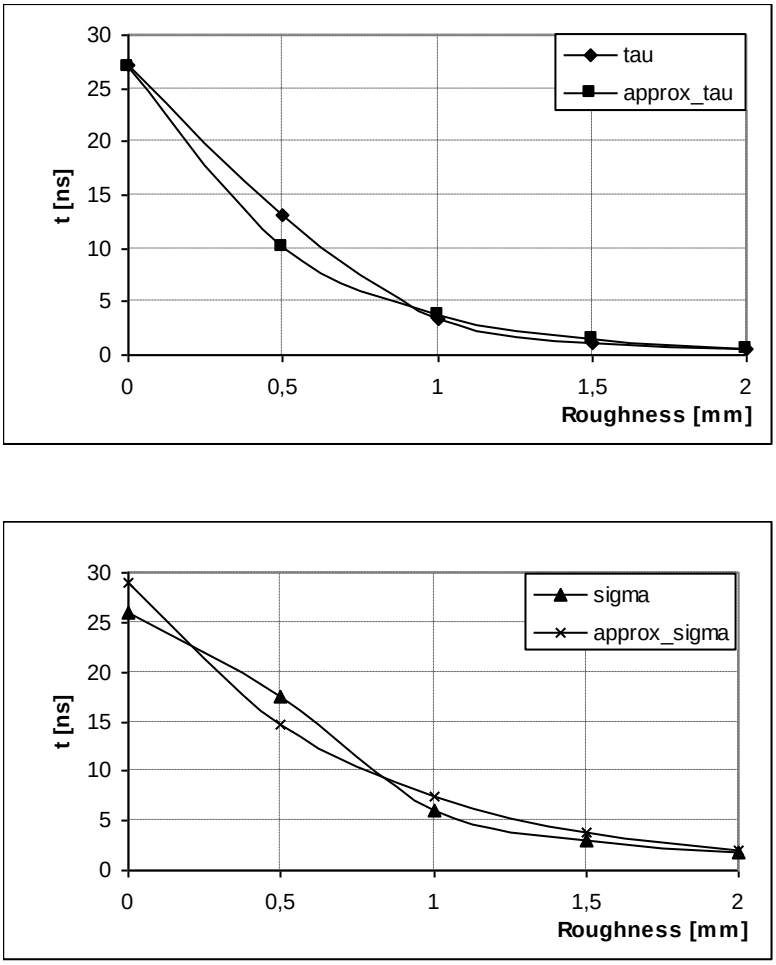

Figure 3.12 Approximation of delay parameters by exponential function of reflecting surfaces roughness

3.5 Dependence on the width of the street

Simulations have been done for the following conditions:

1. changes of the street width in the range [3 , 50] m
2. other scenario parameters as in the standard street (for situations when W<10 m the receiver has been positioned on the street middle, in other cases 3,5 m from the wall)

Results of simulations are presented in Fig.3.13. When the width of the street increases the channel is more dispersive (slope of the profile is smaller, so it is moved up). It is caused by the increase of the path length difference between the direct and reflected rays. The length of the direct ray for each MS position along the street is not changed, but the lengths of rays reflected from walls increase for wider street. So these components are more delayed and have almost the same amplitude (changes of the length are small for higher attenuation of the signals), and the profile is moved up.

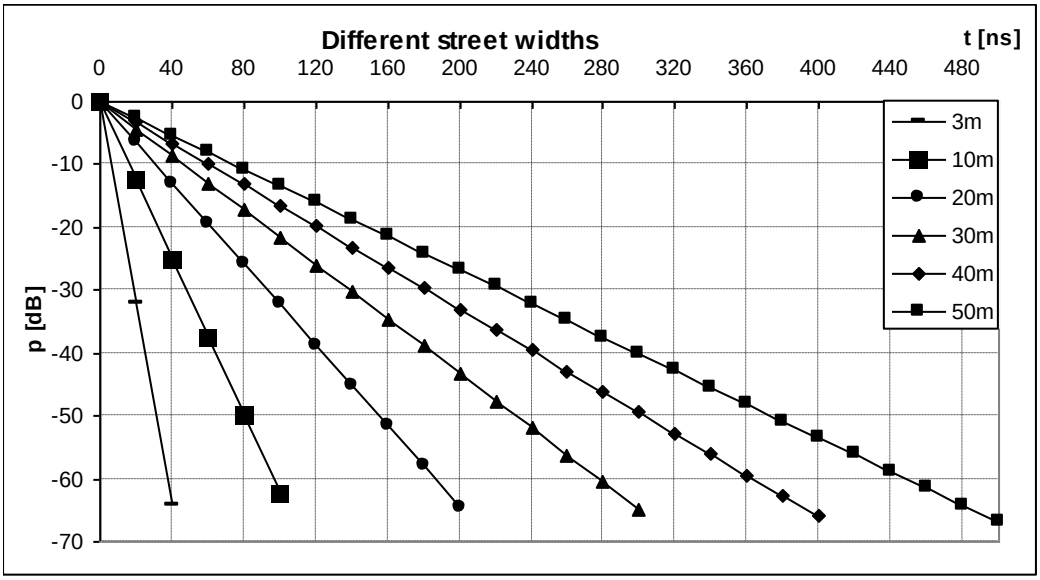

Figure 3.13 Power delay profiles for different streets widths

Delay parameters are presented in Tab.3.5 and in Fig.3.14. They are very sensitive on the street width and change from single ns for the narrow street to about thirty ns for the 50 m wide street. When the width increases five times, mean delay increases above seven times and delay spread increases above five times. Dependence of mean delay and delay spread on the street width, for the considered range of widths, can be described by a power function:

$$\sigma = a \cdot W^{b} \qquad (3.12)$$

where *a* and *b* constants depended on other scenario parameters; the value of *b* is larger than one.

For the simulations that have been done these functions are:

$$\tau = 0{,}158W^{1{,}32} \tag{3.13}$$

$$\sigma = 0{,}52W^{1{,}07} \tag{3.14}$$

where:

mean delay τ and delay spread σ are in ns

W - the street width in m

W [m]	Mean deay [ns]		Delay spread [ns]	
	simul. prof. τ	approx. prof. τ_approx	symul. prof. σ	approx. prof. σ_approx
3	0,66	0,94	2,07	2,36
5	1,34	2,02	2,93	3,76
10	3,33	4,75	6,14	6,80
20	8,25	11,13	12,86	13,40
30	13,61	17,69	19,23	20,03
40	20,66	23,91	27,15	26,30
50	26,33	29,85	35,06	32,14

Table 3.5 Delay parameters for different streets widths

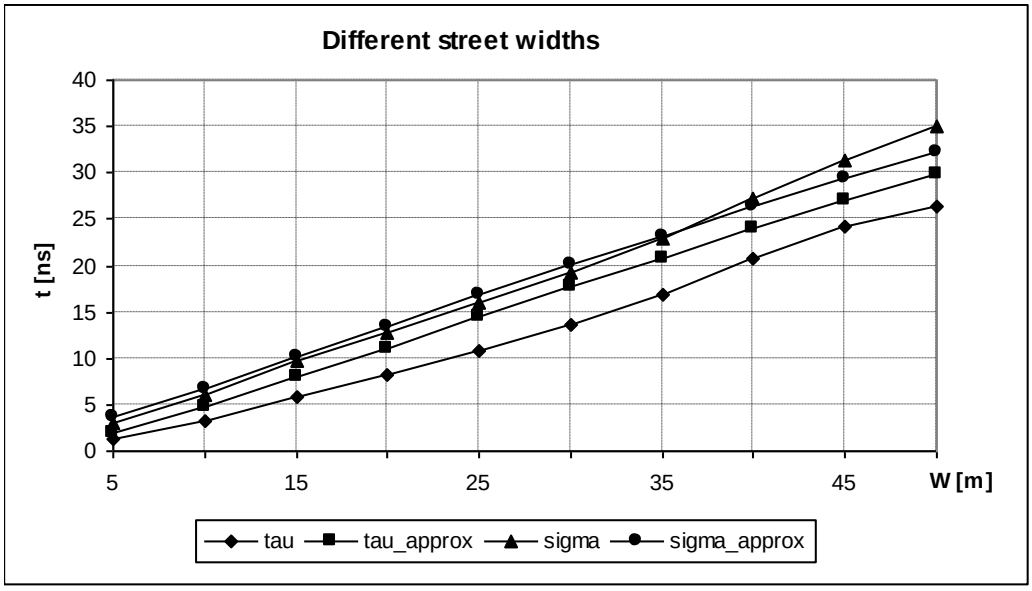

Figure 3.14 Delay parameters for different streets widths

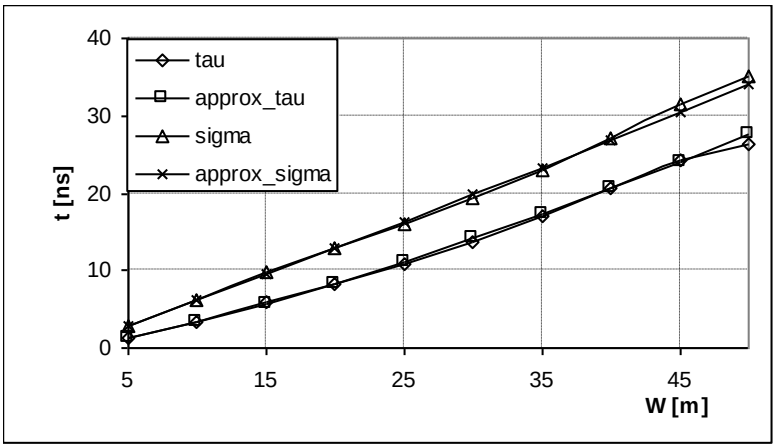

Figure 3.15 Approximation of delay parameters by power function of the streets width

Delay parameters obtained from simulations and their approximations given by (3.13) (3.14) are presented in Fig.3.15. These approximations give values almost identical with calculated values.

3.6 Dependence on the length of the street

Simulations have been done for changes in the street length in the range [100 , 1000] m. Results are presented in Fig.3.16.

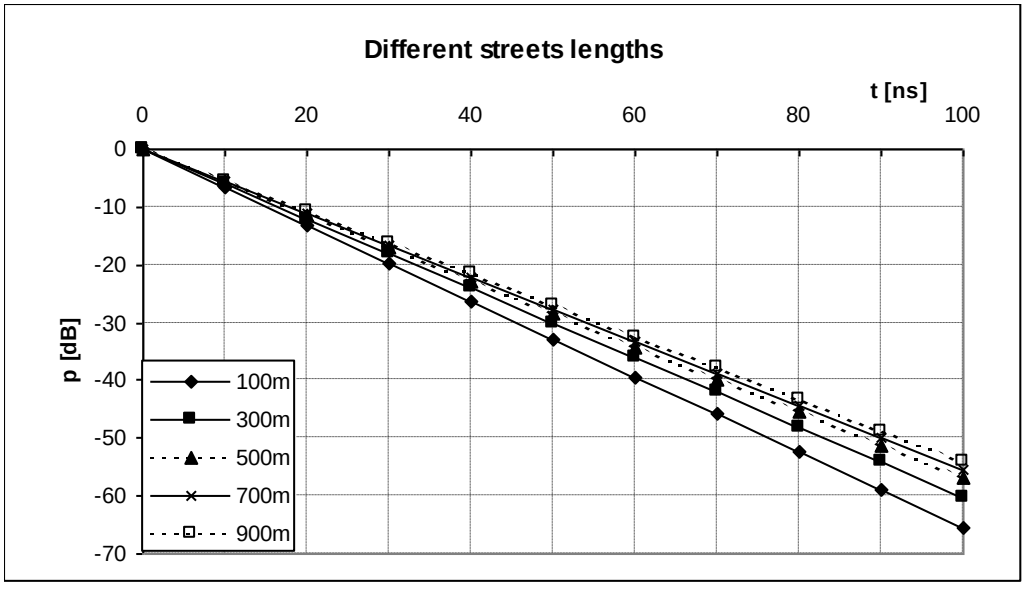

Figure 3.16 Power delay profiles for different streets lengths

When the distance between the transmitter and the receiver is large, the reflected components have small delays to the direct ray. For example for the simulated street (10 m wide and 200 MHz system bandwidth) when the distance is longer than 300 m all reflected rays and direct ray arrive at the receiver in the same delay beam (the discrete delay profile has only one direct component). Due to a longer path, these components are highly attenuated, which causes that the averaged received power along the street in each delay beam is smaller for small delays (specially for direct beam). This effect causes a larger importance of the higher delay components in the power delay profile for longer streets (due to normalizing to the smaller direct component).

Calculated delay parameters are presented in Table 3.6 and in Fig.3.17. They are larger for a longer street (due to the decrease of power of the direct beam), but when the street is ten times longer mean delay τ increases about two times, others parameters: delay spread σ and σ_{approx} and τ_{approx}, calculated from exponential approximation, increase in a smaller range.

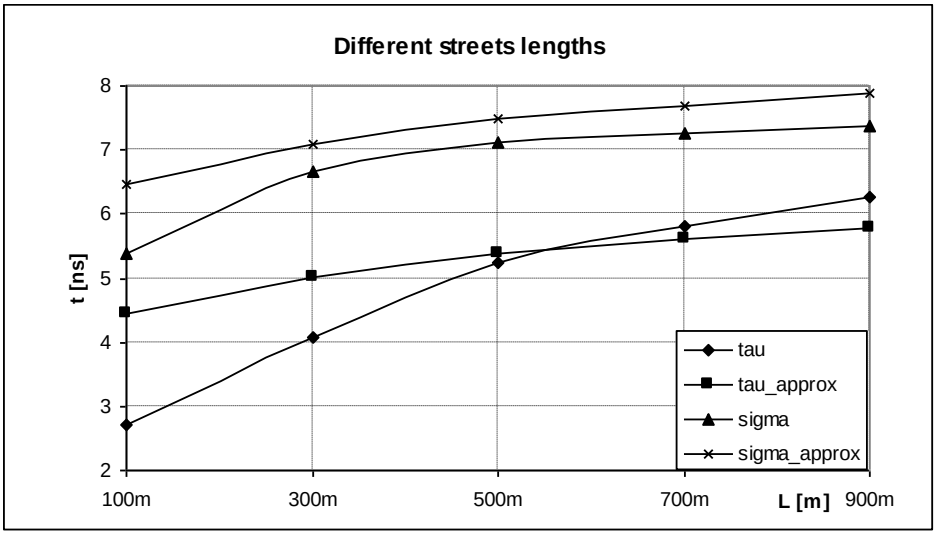

Figure 3.17 Delay parameters for different streets lengths

L [m]	Mean deay [ns]		Delay spread [ns]	
	simul. prof. τ	approx. prof. τ_approx	symul. prof. σ	approx. prof. σ_approx
100	2,71	4,44	5,38	6,47
300	4,09	5,01	6,65	7,08
500	5,24	5,40	7,12	7,49
700	5,80	5,60	7,27	7,70
900	6,27	5,78	7,36	7,89

Table 3.6 Delay parameters for different streets lengths

The dependence of delay parameters on the street length (for the considered range of changes) can be described by a power function (similar as the one for different widths of the street, but in this case *b* is much smaller than one):

$$\sigma = a \cdot L^{b} \tag{3.15}$$

where *a* and *b* constants depended on scenario parameters.

For the simulated street scenario, delay parameters are described by:

$$\tau = 0{,}51 L^{0{,}31} \tag{3.16}$$

$$\sigma = 3{,}2\, L^{0{,}13} \tag{3.17}$$

where:

mean delay τ and delay spread σ are in ns

L - the street length in m

Results of these approximations are presented in Fig.3.18. For τ the approximation is very good , and for σ there are some differences for small and large value of the street length, but they are smaller than 10%.

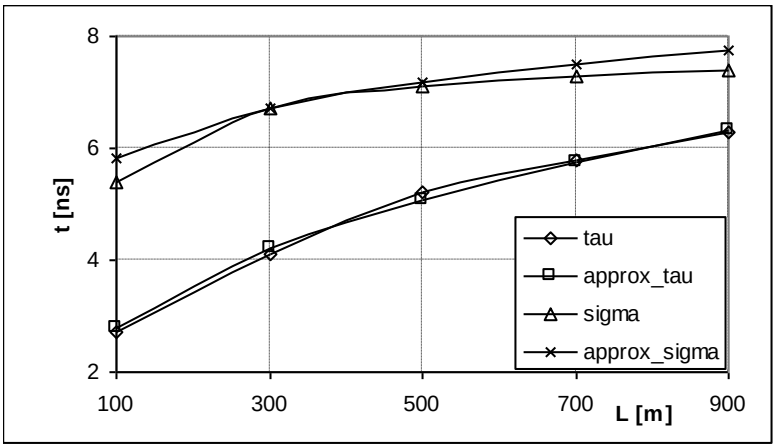

Figure 3.18 Approximation of delay parameters by power function of the streets length

3.7 Dependence on base and mobile stations position

To determine the influence of the transmitter and the receiver position in the diagonal street plane on the delay parameters of the channel, the following simulations have been done:

1. Changes of BS distance from the wall.
2. Changes of MS position from the wall.

The transmitter or the receiver have been placed from near a wall to the middle of the street. The obtained power delays profiles for different positions of the BS are presented in Fig.3.19. When the transmitter is near the wall, the delay of rays reflected from the other wall is larger, so in this case the profile is moved up (slope is smaller).

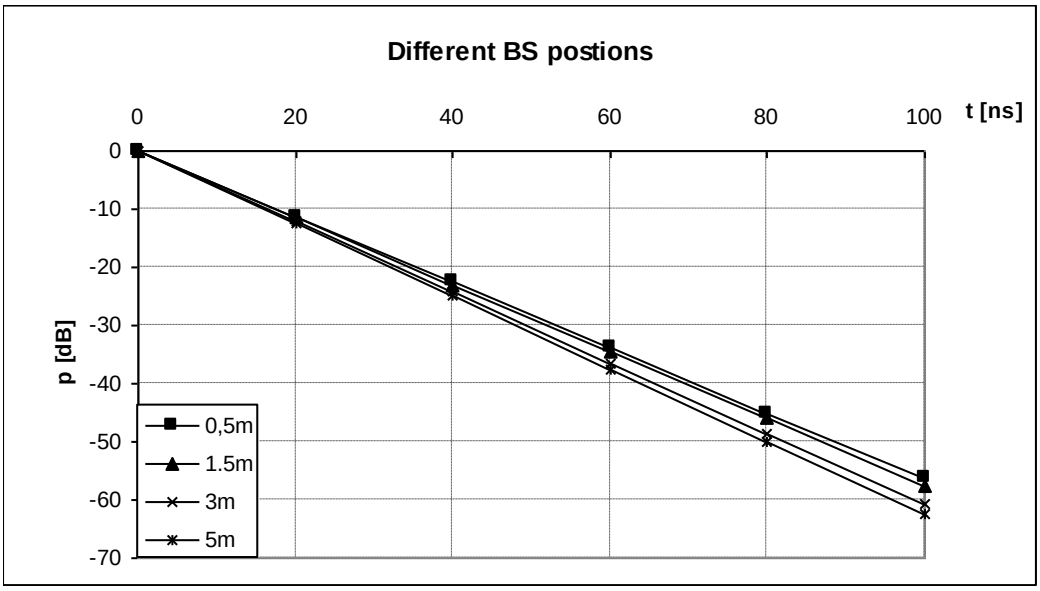

Figure 3.19 Power delay profiles for different BS positions

When the BS is not on the street middle there are two cases for the MS position: either it is on the same side of the street or it is on other one. These situations are not significantly different, but slightly better results are obtained when the receiver and the transmitter are on the same side of the street, specially for the BS near the wall. In this case first order reflected ray from this wall has a larger amplitude ($\Gamma \approx 1$ because the angle of incidence is near zero) and very small delay to the direct ray (smaller than the delay beam), so they are received by the receiver as one signal with higher amplitude and the importance of delayed rays is smaller. When the receiver is on the other side of the street this reflected ray arrives to the receiver in a different delay beam than the direct ray.

Mean delay and delay spread are presented in Tab.3.7 and in Fig.3.20. They are larger when BS is nearer the wall. When the BS changes position from near a wall to the middle of the street τ decrease from 5 to 3,3 ns, and σ decreases from 8 to 6 ns. Changes of these parameters can be described by a linear function of the BS distance from the wall.

d_BS [m]	Mean deay [ns]		Delay spread [ns]	
	simul. prof. τ	approx. prof. τ_approx	symul. prof. σ	approx. prof. σ_approx
0,1	4,93	5,57	7,92	7,67
1	4,70	5,45	7,47	7,55
2	4,06	5,12	6,90	7,20
3	3,50	4,95	6,69	7,02
4	3,43	4,84	6,30	6,90
5	3,33	4,75	6,14	6,80

Table 3.7 Delay parameters for different BS positions

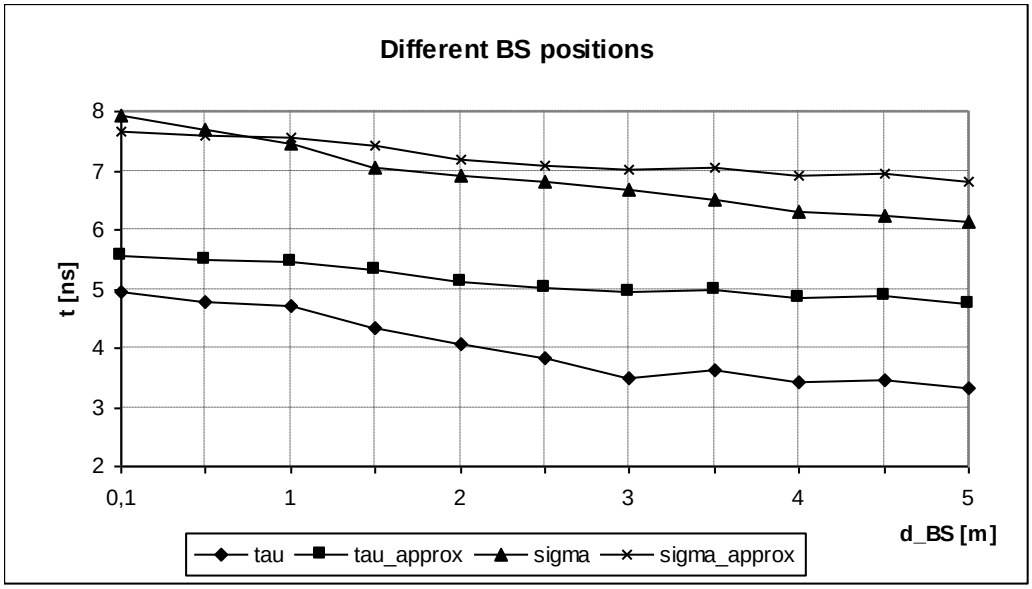

Figure 3.20 Delay parameters for different BS positions

For the street considered in the simulations these dependencies are given by:

$$\tau = -0{,}33 d_{BS} + 4{,}9 \tag{3.18}$$

$$\sigma = -0{,}39 d_{BS} + 7{,}9 \tag{3.19}$$

where:

mean delay τ and delay spread σ are in ns

d_{BS} - the BS distance from the wall in m

These approximations are presented in Fig.3.21 and as it is seen they give a good accuracy and can be used to describe changes of delay parameters caused by changes of the BS position.

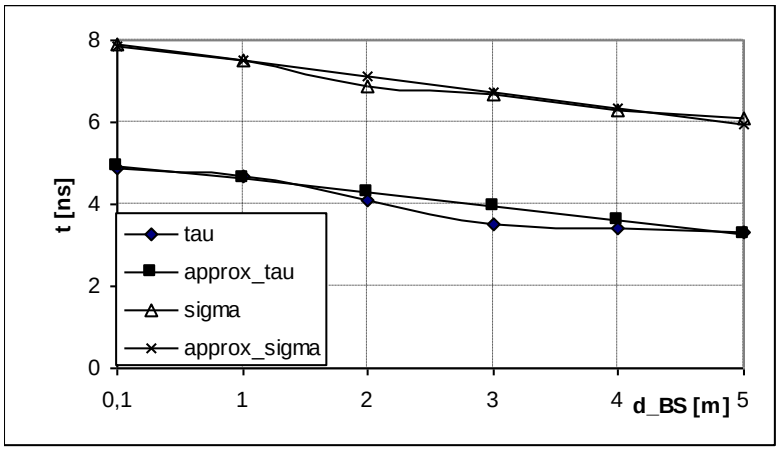

Figure 3.21 Approximation of delay parameters by linear function of the BS position

Results for different MS positions are presented in Fig.3.22. The profiles are almost independent of this parameter, excepted in situation when the receiver is on middle of the street (in the symmetric scenario because the BS is on the middle too). In this case, rays reflected from both walls (mirror reflection) have the same delay (coming in the same delay beam) and power received in this beam is larger, so the slope of the profile decreases. When the receiver is not in the street middle these rays have different delays (coming in different delay beams when the path length difference is larger than 1,5 m for a system bandwidth of 200 MHz - time resolution of the system 5 ns). For changes on the MS position the results obtained are different from those corresponding to changes on the BS position because the transmitter and the receiver have different antennas heights, so these situations are not symmetric for multiple reflected rays with last reflection from the ground.

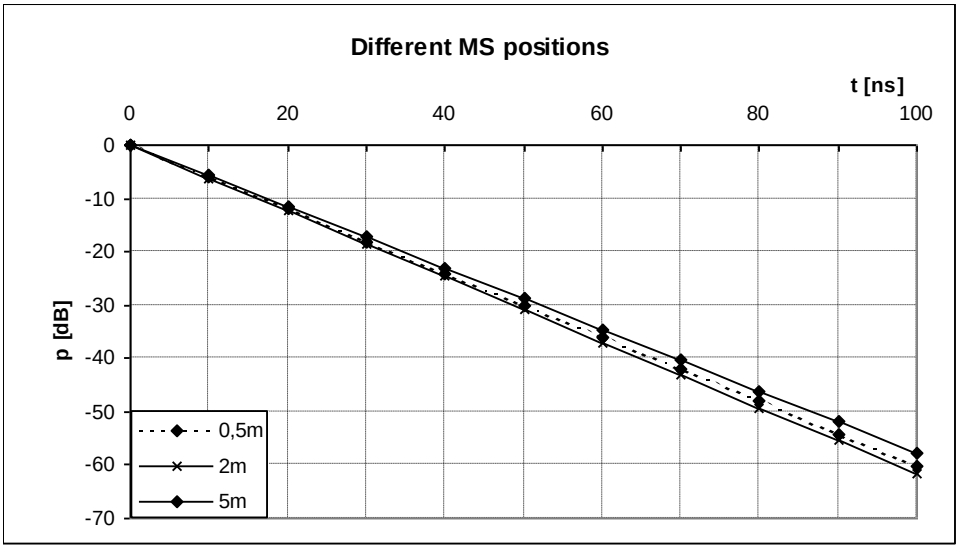

Figure 3.22 Power delay profiles for different MS positions

Calculated delay parameters are presented in Tab.3.8 and are almost constant when a distance of the MS from wall changes, Fig.3.22 (excluding situation when the MS is in the middle of the street; in this case these parameters are larger).

d_MS [m]	Mean deay [ns]		Delay spread [ns]	
	simul. prof. τ	approx. prof. τ_approx	symul. prof. σ	approx. prof. σ_approx
0,5	3,47	5,01	6,47	7,08
1	3,58	4,93	6,58	6,99
2	3,42	4,84	6,27	6,90
3	3,23	4,87	6,12	6,93
4	3,41	4,81	6,21	6,87
5	4,12	5,30	6,75	7,39

Table 3.8 Delay parameters for different MS positions

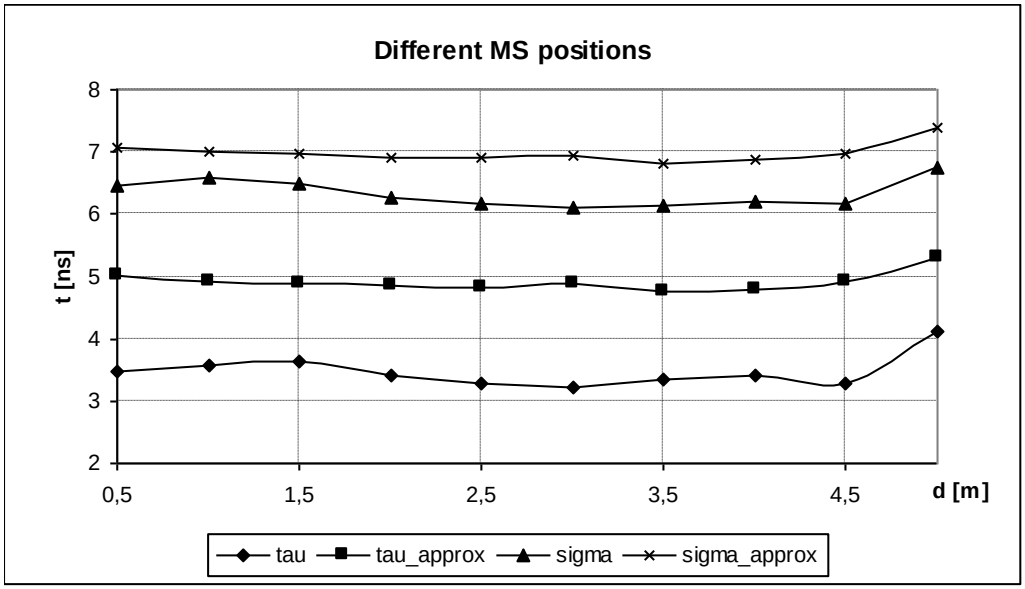

Figure 3.23 Delay parameters for different MS positions

3.8 Dependence on base and mobile stations antennas' heights

The following simulations have been done:

1. changes on the BS antenna height in the range [5, 30] m
2. changes on the MS antenna height in the range [1, 3] m

Power delay profiles for different BS antenna heights are presented in Fig.3.24. When the height increases the profile is moved down, because the direct distance between BS and MS antennas increases and delays of reflected rays are smaller (multiple reflected from the walls components have larger delays).

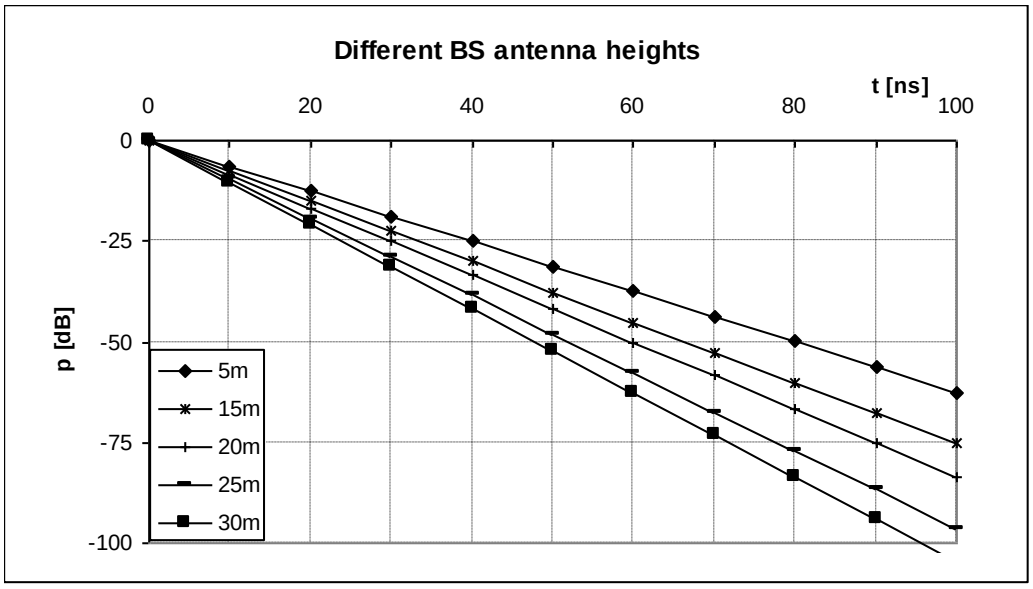

Figure 3.24 Power delay profiles for different BS antenna heights

Delay parameters are presented in Tab.3.9 and in Fig.3.25. They decrease when the BS antenna height increases: mean delay τ in the range [2,5, 3,5] ns and delay spread σ in the range [5, 6,5] ns when the antenna height varies from 30 to 5 m. The dependence of these parameters on the BS antenna height can be approximated by a linear function. For the simulated street these are:

$$\tau = -0{,}023 h_{BS} + 3{,}4 \qquad (3.20)$$

$$\sigma = -0{,}049 h_{BS} + 6{,}4 \qquad (3.21)$$

where:

mean delay τ and delay spread σ are in ns

h_{BS} - the BS antenna height in m

Results of these approximations are presented in Fig.3.26.

h_BS [m]	Mean deay [ns]		Delay spread [ns]	
	simul. prof. τ	approx. prof. τ_approx	symul. prof. σ	approx. prof. σ_approx
5	3,33	4,75	6,14	6,80
10	3,45	4,12	5,78	6,13
15	3,21	3,63	5,54	5,59
20	3,06	3,10	5,36	5,01
25	2,87	2,46	5,17	4,28
30	2,74	2,14	4,93	3,91

Table 3.9 Delay parameters for different BS antenna heights

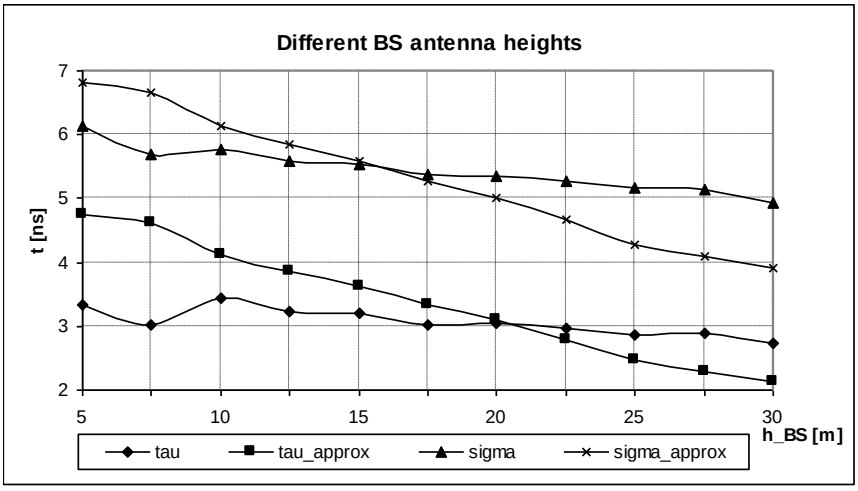

Figure 3.25 Delay parameters for different BS antenna heights

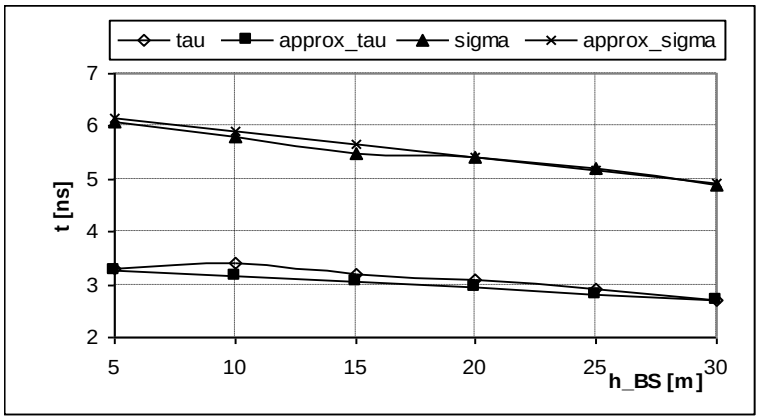

Figure 3.26 Approximation of delay parameters by linear function of the BS antenna height

Power delays profiles for different MS antenna heights are presented in Fig.3.27. In this case the slope of the profile is larger for lower antenna positions because the direct distance between both antennas increases (inversly as for changes of the BS antenna height), which causes that rays reflected from the wals have smaller delays. Additionaly for a lower antenna height the length of the ray reflected from the ground is smaller. Delay parameters are presented in Tab.3.10 and they increase with the MS antenna height increasing, but these changes are so small that parameters τ and σ can be considered as constants or as linear function of the MS antenna height (considered changes of h_{MS} in the range [, 2 m):

$$\tau = 0{,}13 h_{MS} + 3{,}2 \tag{3.22}$$

$$\sigma = 0{,}175 d_{MS} + 5{,}9 \tag{3.23}$$

where:

mean delay τ and delay spread σ are in ns

h_{MS} - the MS antenna height in m

These approximations are presented in Fig.3.28. Delay parameters increase slightly when the MS antenna height increases (excluding the case when $h_{MS} \approx 1\text{m}$).

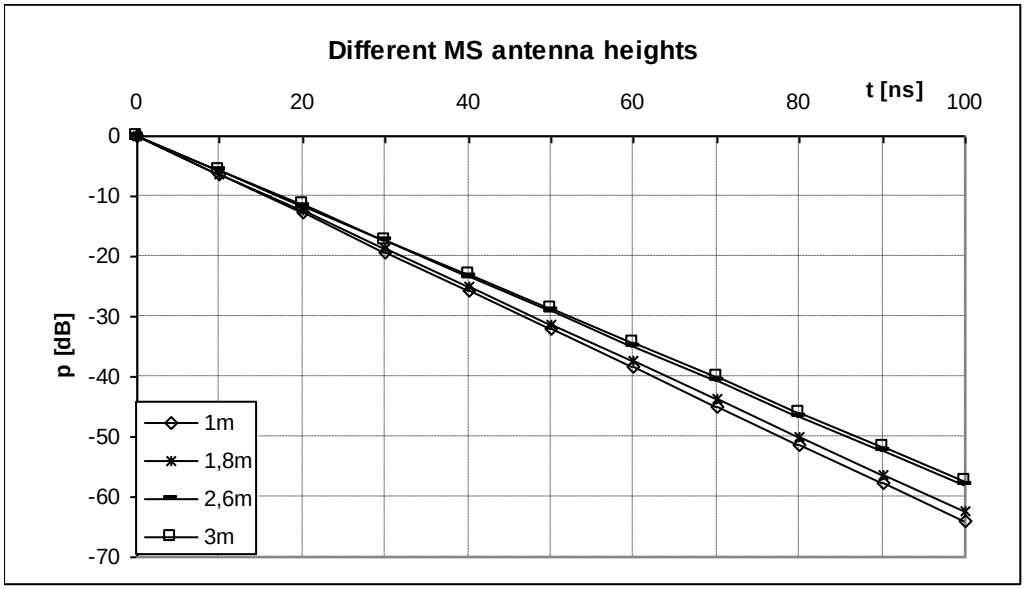

Figure 3.27 Power delay profiles for different MS antenna heights

h_MS [m]	Mean deay [ns]		Delay spread [ns]	
	simul. prof. τ	approx. prof. τ_approx	symul. prof. σ	approx. prof. σ_approx
1	3,68	4,58	6,26	6,62
1,4	3,29	4,74	6,12	6,80
1,8	3,33	4,75	6,14	6,80
2,2	3,41	5,16	6,29	7,24
2,6	3,45	5,25	6,33	7,33
3	3,64	5,34	6,57	7,43

Table 3.10 Delay parameters for different MS antenna heights

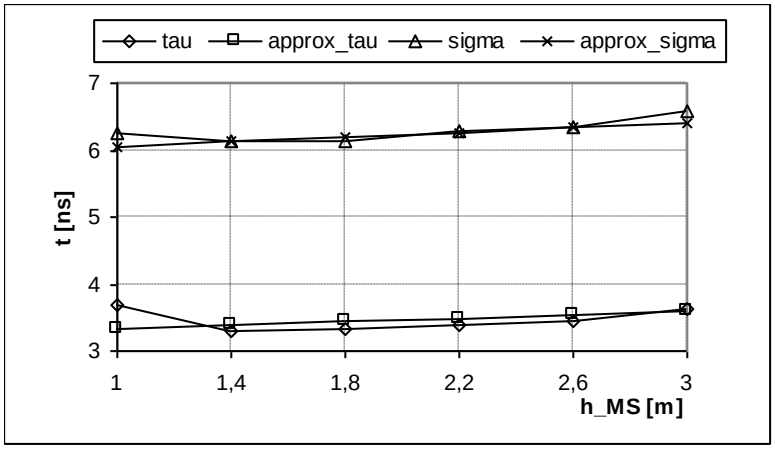

Figure 3.28 Approximation of delay parameters by linear function of the MS antenna height

3.9 Dependence on antennas types

Simulations for different types of antennas, both BS and MS, have been done. The propagation scenario has been considered as the standard street, and the following types of antennas have been considered:

1. isotropic antenna - the same gain in every directions
2. lower - isotropic in the lower hemisphere BS antenna, and zero everywhere else
3. upper- isotropic in the upper hemisphere MS antenna, and zero everywhere else
4. ideal - BS antenna, which allows to obtain an equal received power independent of the distance between MS and BS (omnidirectional in the horizontal plane)

5. MBS antenna - special type of antenna for BS and MS, allowing to obtain the equal received power along the street and attenuate reflected rays [24](radiation patterns used in simulations are presented in Annex A). It is an antenna with fixed orientation: in the BS it looks down and in the MS it looks up (BS antenna height is higher than MS antenna height)
6. directive - antenna with narrow beam; the pattern of this antenna used in simulation is presented in Annex A (the same in both planes). This antenna must change its orientation when the receiver moves along the street, and it intends to simulate an adaptive array antenna at the MS.

Fig.3.29. presents power delay profiles for different antennas types. The worst case is when both antennas are isotropic, the rays transmitted and received from different directions having the same gain. Using other types of antenna, with more directional patterns, it is possible to eliminate some multipath components. The upper antenna in the MS does not receive components reflected from the ground (which come from lower hemisphere), so the profile is moved down. Another improvement of the channel properties can be obtained by using the ideal antenna in the transmitter. Signals for the small distances between BS and MS are less "amplified" by this antenna (these signals produce large delays components of the profile) in comparison with signals for larger distances, so their influence on the profile is smaller. The best results are obtained for directional antennas: MBS and 20^{o} beamwidth directive antenna, these antennas allow to eliminate or highly attenuate multipath components. Best results obtained for MS antennas are caused by additional attenuation of signals for small distances between the receiver and the transmitter (like ideal antenna), so the contribution of these components to the average power delay profile is smaller. The disadvantage of the beam directive antenna is that it must follow the source of the signal by changing its orientation when MS moves along the street.

Using directive antennas, properties of the channel can be improved, but there can be problems when the direct ray is obstructed by trees, big cars or other obstacles. In this case communications can be lost, because the power of received multipath components can be to small to enable the proper functioning of the receiver.

Delay parameters are presented in Tab.3.11. They vary in the range from fractions of ns for the MBS antennas to few ns for isotropic antennas, which means that influence of antennas types on the channel properties is high.

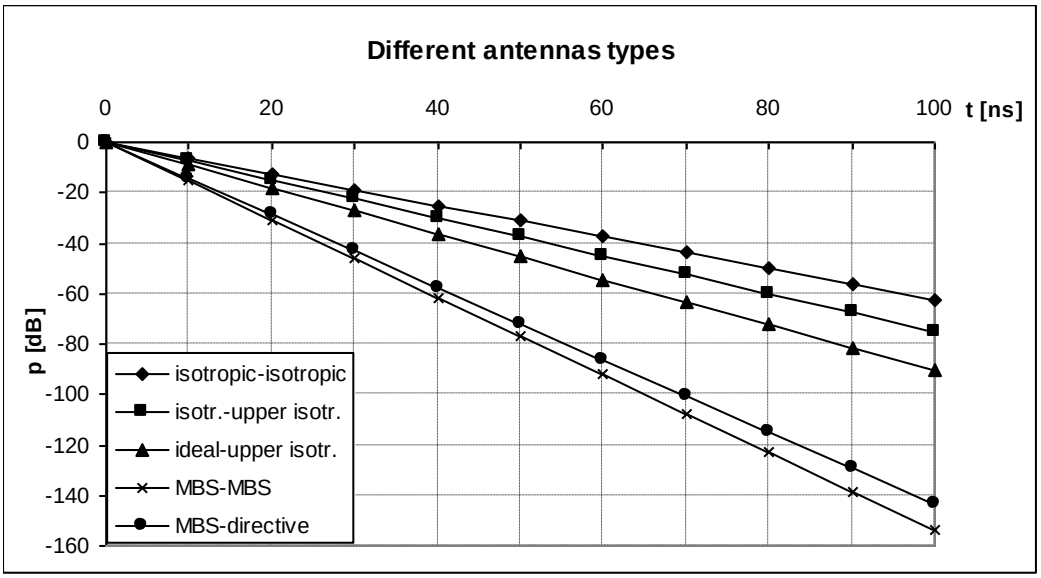

Figure 3.29 Power delay profiles for different types of BS and MS antennas

BS-MS antennas	Mean deay [ns]		Delay spread [ns]	
	simul. prof. τ	approx. prof. τ_approx	symul. prof. σ	approx. prof. σ_approx
isotropic-isotropic	3,33	4,75	6,14	6,80
isotropic-upper	3,58	3,65	5,71	5,62
lower-isotropic	3,33	4,75	6,15	6,80
lower-upper	3,58	3,65	5,71	5,60
ideal-isotropic	3,43	4,25	5,54	6,27
ideal-upper	2,37	2,73	4,25	4,59
MBS-MBS	0,01	0,98	0,12	2,43
MBS-directive	0,38	1,33	1,53	2,90

Table 3.11 Delay parameters for different types of BS and MS antennas

3.10 Dependence on traffic in the street

Simulations for traffic on the street have been done in order to determine its influence on the propagation channel properties. It has been used a simple model of the street full of cars: metal surface 1,5 m above the ground (by decreasing in the simulation scenario the antennas heights). Obtained profiles for street without traffic and with traffic are presented in Fig.3.30. The metal surface causes an increase on the amplitude of the rays, that reflected

from it (specially for small distance between the receiver and the transmitter), but appropriate decreasing of the antennas heights (smaller path length for the ray reflected from the ground) compensate this effect (specially the MS antenna, which in this case is only 0,3 m above the ground surface. The delays parameters are presented in Tab.3.12. Values of parameters calculated from simulation profile are slightly larger for traffic on the street due to larger power for small delays in this case.

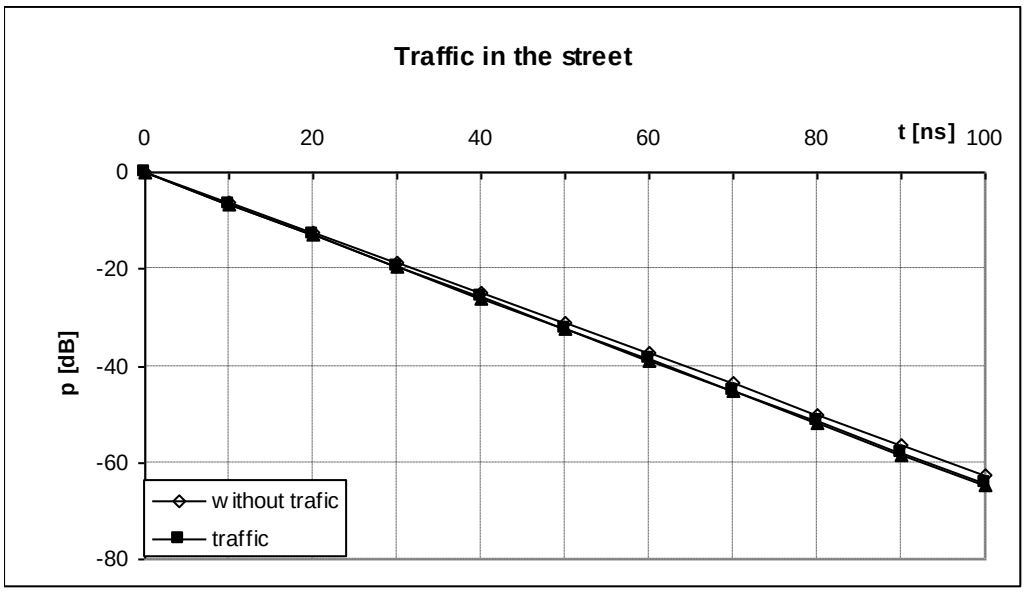

Figure 3.30 Power delay profiles for traffic in the street

	Mean deay [ns]		Delay spread [ns]	
	simul. prof. τ	approx. prof. τ_approx	symul. prof. σ	approx. prof. σ_approx
without traffic	3,33	4,75	6,14	6,80
traffic	3,70	4,56	6,37	6,60

Table 3.12 Delay parameters for traffic in the street

4. Conclusions

An analysis of the wideband propagation channel in MBS has been presented. The simulations have been done using a geometrical optics approach and considering a typical propagation scenario: an urban street with buildings on both sides. The dependencies of the delay parameters (mean delay and delay spread) used to characterize the dispersive nature of the channel on different propagation scenario conditions have been considered, and approximations to these dependencies have been developed. Tab.4.1 presents the considered scenario parameters, the ranges of their changes, the values of the delay parameters and the types of dependencies.

Dependence on	Range of changes	Mean deay τ [ns]		Delay spread σ [ns]		Approximation function of delay parameters
		min.	max.	min.	max.	
System bandwidth	[20,1000]MHz	0,02	6,8	0,9	7,5	hyperbolic tangents
Street width	[3,50]m	0,7	26,3	2,1	35,1	power (increasing)
Street length	[100,1000]m	2,7	6,3	5,4	7,4	power (increasing)
Roughness of walls	[0,2]mm	0,6	27,2	1,8	26,0	exponential (decreasing)
BS antenna height	[5,30]m	2,7	3,3	4,9	6,1	linear (decreasing)
MS antenna height	[1,3]m	3,3	3,7	6,1	6,6	linear or constant
BS position	[0,5]m	3,3	4,9	6,1	7,4	linear (decreasing)
MS position	[0,5]m	3,5	4,1	6,2	6,7	constant
Walls materials		2,1	3,3	4,6	6,2	
Antennas types		0,01	3,3	0,1	6,1	
Traffic		3,3	3,7	6,1	6,4	

Table 4.1Considered scenario parameters and their influence on delay parameters

Delay parameters depend on the system bandwidth: for wideband systems the channel is more dispersive and parameters have larger values, the dependence being approximated by an hyperbolic tangent function. Delay parameters increase when the width and length of the street are larger, but the channel is more sensitive to changes of the street width rather than its length; these dependencies can be approximated by a power function. The influence of the BS and the MS positions and antennas heights on the delay parameters can be approximated by a linear function, the most influent parameters being the BS antenna height (it can vary in the large range). Generally when the BS antenna is high or near the middle of the street the delay

parameters are smaller. These parameters are less sensitive to changes in the MS position and antenna height, and as a first approximation they can be considered as constants (changes caused by the MS antenna height variation can be approximated by a linear function, parameters increasing for larger antenna heights). The types of used antennas has influence on the delay parameters: directional antennas allow to eliminate reflected rays and the channel is less dispersive. Additional influence on the channel properties comes from the roughness of the reflecting surfaces; for rough surfaces, the amplitudes of reflected rays decrease very fast. The dependence of the delay parameters on the roughness can be approximated by an exponential function. The influence of the electrical parameters of the reflecting surfaces on the channel properties is small. Results for a street full of cars (modeled by a metal surface 1,5 m above the ground) are almost identical as for an empty street.

In general the delay parameters of the propagation channel are most sensitive to:

1. width of the street
2. bandwidth of the receiver
3. types of the used BS and MS antennas
4. roughness of reflecting surfaces
5. BS antenna height (if it changes in a large range)

Other scenario conditions have a smaller influence on the channel properties.

Annex A. Radiation patterns of antennas used in simulations

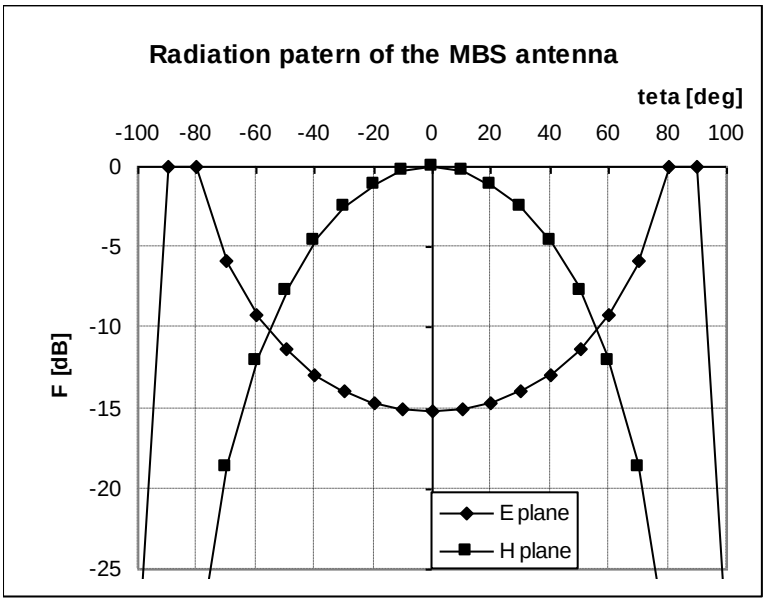

Figure A.1 Radiation paterns in E plane (along the street) and H plane of the MBS antenna used in simulations

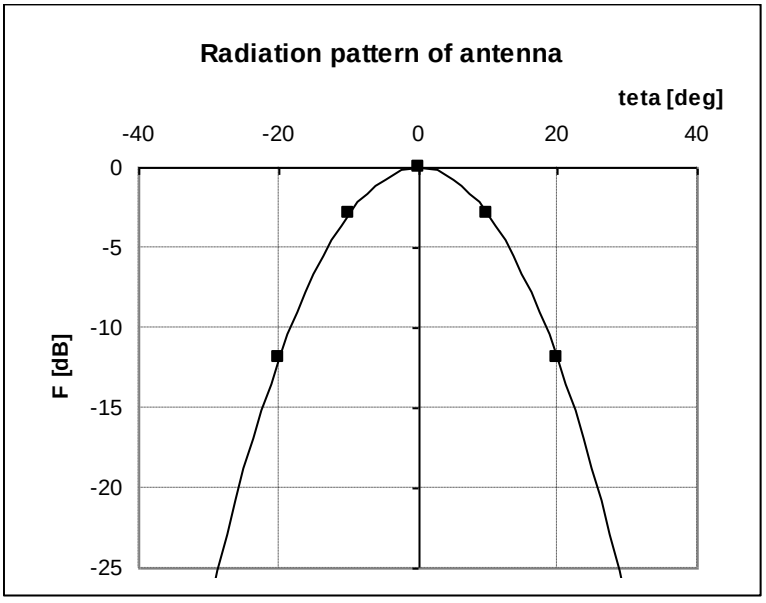

Figure A.2 Radiation pattern of the directive antenna with 20^{o} beamwidth in both planes, used in simulations

References

[1] J. S. Dasilva, D. Ikonomou, H. Erben, "European R&D Programs on Third-Generation Mobile Communications Systems", *IEEE Personal Communications,* Vol. 4, No. 1, Feb. 1997, pp.46-52

[2] L. Fernandes, "R2067 MBS - Mobile Broadband System", *Proceedings of ICUPC'93 2nd IEEE International Conference on Universal Personal Communications*, Ottawa, Canada, Oct. 1993

[3] L. Fernandes, "R2067 MBS A System Concept and Technologies for Mobile Broadband Communications", *Proceedings of RACE Mobile Telecommunications Summit*, Cascais, Portugal, Nov. 1995

[4] G. Calhoun, *Digital Cellular Radio,* Artech House, Norwood, MA, USA, 1988

[5] T. H. Rappaport, *Wireless Communications: Principles and Practices*, IEEE Press, Piscataway, NJ, USA, 1996

[6] http::/www.baltzer.nl/wirelesscd/

[7] K. Pahlavan, A. H. Levesque, *Wireless Information Networks*, Willey, New York, USA, 1995

[8] R. Steele, *Mobile Radio Communications,* Pentech Press, London, UK, 1992

[9] M. Lu , T. Lo, J. Litva, " A Phisical Spatio-Temporal Model of multipath Propagation Channels", *Proceedings of VTC'97 - 47th IEEE Vehicular Technology Conference*, Phoenix, USA, May 1997

[10] I. D. Parsons, *The Mobile Radio Propagation Channel*, Pentech Press, London, UK, 1992

[11] L. Correia (ed.), "*Final Report of Propagation Aspects*", RACE-MBS Deliverable R2067/IST/2.2.5/DS/P/070.b1, European Commission, DG XIII/B, Brussels, Belgium, Dec. 19995

[12] M. D. Yacoub, *Foundations of Mobile Communications*, CRC Press, Boca Raton, Florida, USA, 1993

[13] G. L. Stuber, *Principles of Mobile Communications,* Kluwer, Boston, USA ,1996

[14] R. H. Clarke, "A statistical Theory of Mobile Radio Reception", *Bell System Technical Journal,* Vol. 44, 1968, pp. 957-1000

[15] P. Vasconcelos, L. Correia, "Fading Characterization of the Mobile Radio Channel at Millimetre Waveband", *Proceedings of VTC'97 - 47th IEEE Vehicular Technology Conference*, Phoenix, USA, May 1997

[16] W. Mohr, "Modeling of Wideband Mobile Radio Channels Based on Propagation Measurements", *Proceedings of PIMRC - 7th IEEE International Symposium on Personal Indoor and Mobile Radio Communications*, Toronto, Canada, Sep. 1995

[17] I. Oppermann, B. White, B. S. Vucetic, "Wide-Band Fading Channel Model for Micro-Cellular Systems", *Proceedings of PIMRC - 7th IEEE International Symposium on Personal Indoor and Mobile Radio Communications*, Toronto, Canada, Sep. 1995

[18] L. Correia, J. Reis, "Wideband Characterization of the Propagation Channel at 60 GHz", *Proceedings of PIMRC - 7th IEEE International Symposium on Personal Indoor and Mobile Radio Communications*, Taypey, Singapure, Oct. 1996

[19] A. Kanatas, I. D. Kountouris, G. B. Kostaras, P. Constantinou, "A UTD Propagation Model in Urban Microcellular Environments", *IEEE Transaction on Vehicular Technology*, Vol. 46, No. 1, Feb 1997, pp. 185-193

[20] L. Correia, P. O. Frances, "The MBS Path Loss Model for Outdoor Scenarios", *Proceedings of RACE Mobile Telecommunications Workshop*, Amsterdam, The Netherlands, May 1994

[21] "Attenuation by Atmospheric Gases", *Recomendation and Reports of the CCIR*, Rep. 719-2, Vol. V (Propagation in Non-Ionized Media), ITU, Geneva, Switzerland, 1986, pp. 167-177

[22] "Attenuation by Hydrometeors, in Particular Precipation, and Other Atmospheric Particles", *Recomendation and Reports of the CCIR*, Rep. 719-2, Vol. V (Propagation in Non-Ionized Media), ITU, Geneva, Switzerland, 1986, pp. 199-214

[23] J. J. Reis, L. M. Correia, "*Propagation Model for Outdoor Mobile Communications at Millimetre Waveband in Urban Scenarios",* Internal Report, MBS/WP.2.2.3/IST085.1 IST, Lisbon, Portugal, Nov. 1994

[24] C. A. Fernandes, P. O. Frances, A. M. Barbosa, *"Test Report on Antennas Assemblies",* RACE-MBS Deliverable R2067/IST/4.6.2/DS/P/041.b1, European Commission, DG XIII/B, Brussels, Belgium, Dec. 1994